SURGICAL FLUORESCENCE IMAGER FOR VISUALIZING ANTERIORLY PLACED BILIARY STRUCTURES, *IN-VIVO* DURING HUMAN CHOLECYSTECTOMY

BY

SANTOSH HARIHARAN

Presented to the Faculty of Graduate School of

The University of Texas at Arlington in Partial Fulfillment

Of the Requirements

For the degree of

MASTER OF SCIENCE IN BIOMEDICAL ENGINEERING

THE UNIVERSITY OF TEXAS AT ARLINGTON

August 2008

ACKNOWLEDGEMENTS

I would like to express my gratitude to all those who helped me for this project. First of all I would like to show my gratitude to Dr. Edward Livingston, Chair of Surgery University of Texas Southwestern Medical Center at Dallas, for providing me with an opportunity and associating himself with this project.

I would like to thank my advisor and mentor Dr. Karel J. Zuzak, Assistant Professor University of Texas Arlington for all the support, encouragement he provided and for his time he has spent with me at every step for the success of this project. It is with his optimistic, enthusiasm and his in-depth knowledge on the subject that made this thesis more exciting for me to work. His sound guidance and teaching made the thesis more interesting

I would like to thank Dr. George Alexandrakis of the Bioengineering department at UTA for his timely, politic advice and guidance for the completion of my work.

I would also like to thank my colleague Mr. Tinsy John Perumanoor for all the help he has provided me during my thesis work. He has been very supportive and encouraging through out my thesis work.

I would like to thank my Brother Mr. Venkatesh Hariharan and my family for all the support and providing me this excellent opportunity to study and work here.Finally thanks to all my friends for being with me through my work.

July 14, 2008

ABSTRACT

SURGICAL FLUORESCENCE IMAGER FOR VISUALIZING ANTERIORLY PLACED BILIARY STRUCTURES, *IN-VIVO* DURING HUMAN CHOLECYSTECTOMY

Santosh Hariharan M.S.

The University of Texas Arlington, 2008

Supervising Professor: Dr. Karel J. Zuzak

Cholecystectomy is one of the most common procedures occurring in United States to cure gall bladder diseases. There are two means of performing this procedure, Open Cholecystectomy and Laparoscopic Cholecystectomy, the later one being more frequent. The critical issue while performing Cholecystectomy is injury to Common Bile Duct (CBD) which could cause post procedural complications. Since the CBD is under fat layer it is important to image and locate the CBD during the procedure. The novel fluorescence imager developed in this project would help visualize the CBD by using the fluorescence properties of Indocyanine Green, to be injected into the body or bilirubin, already existing in bile. The instrument using ICG as a fluorophore has been characterized for its penetration depth to view fluorescence using an intralipid model, determining the best and possible fluorescence concentration that would give maximum fluorescence photons at the same time within the limits of the concentration prescribed for human dosage. The system incorporates a unique combination of short pass-long pass

filter combination at the source and detector end respectively to provide excitation and detect emission. The filters are designed in accordance with the absorption and emission characteristics of individual fluorophore in different medium.

The best fluorescence concentration was found to be 0.015 mg/ml. Depth analysis was performed for ICG mixed with water, going deeper in a 1% intralipid solution used as model to mimic tissue and fat properties. A vernier height gage was coupled to a capillary holder, which held the capillary containing the fluorophore. Two separate analyses were carried out, ICG mixed with human bile and aqueous ICG solution both having an approximate concentration of 0.015 mg/ml. Contrast to background and signal to noise ratio were computed at each depth to find the maximum depth the system can visualize. The maximum depth of penetration was found to be 11 mm below the surface of intralipid when ICG was mixed with bile and 20 mm below the surface for aqueous ICG. The threshold for contrast to background was set based on beef fat measurement.

TABLE OF CONTENTS

LIST OF ILLUSTRATIONS

LIST OF TABLES

Table Page

CHAPTER 1

INTRODUCTION

1.1 Cholecystectomy

Cholecystectomy is one of the most common operations performed in United States. It is frequently used for the treatment of symptomatic gallstones[2]. Cholecystectomy is the surgical removal of gall bladder, a small pear shaped sac that is located directly beneath the liver in the upper right side of the abdomen. Two procedures are utilized to surgically remove the gall bladder are Open Cholecystectomy and Laparoscopic Cholecsytectomy. The laparoscopic method is utilized more frequently. The choice of the procedure is made on individual basis[1]. A Cholecystectomy is performed to treat Cholelithiasis and Cholecystitis. Cholelithiasis is disorders of the extrahepatic biliary tract are related to gallstones. In this condition the gall stones of various shapes and sizes are formed within the gall bladder. Cholecystitis is often caused by Cholelithiasis with choleliths most commonly blocking the cystic duct directly. The gallbladder's wall becomes inflamed. Extreme cases may result in necrosis and rupture. Inflammation often spreads to its outer covering, thus irritating surrounding structures such as the diaphragm and bowel[4]. Cholecystitis usually presents as a pain in the right upper quadrant.

1.1.1 Anatomy

The gallbladder is a small pear-shaped organ that stores and concentrates bile. The gallbladder is connected to the liver by the hepatic duct. It is approximately 3 to 4 inches (7.6 to 10.2 cm) long and about 1 inch (2.5 cm) wide. The function of the gallbladder is to store bile and concentrate. The bile emulsifies fats and neutralizes acids in partly digested food. A muscular valve in the common bile duct opens, and the bile flows from the gallbladder into the cystic duct, along the common bile duct, and into the duodenum (part of the small intestine)[6].

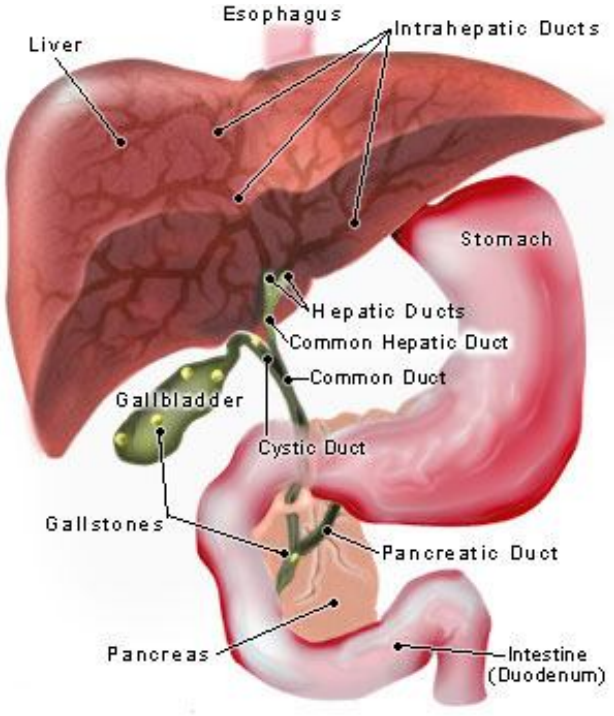

Figure 1.1: Anatomy of Peritoneal Cavity

1.1.2 Disorders with Gall bladder

The following are disorders of the gall bladder:

a. Cholelithiasis: This condition is the presence of stones in gall bladder. Gall stones are bodies formed within the body by accretion or concretion of normal or abnormal bile components.
b. Cholecsytitis: This is the inflammation of gall bladder. Cholecystitis is often caused by Cholelithiasis, with choleliths most commonly blocking the cystic duct directly. The gallbladder's walls become inflamed and could cause further infection and pain resulting from that.
c. Gall bladder Cancer: A relatively uncommon cancer that occurs in the gall bladder. If detected early this could be cured by removing the gall bladder.

1.1.3 Symptoms

Gall bladder diseases are marked with some or all of the following symptoms[7],

1. Pain in the upper right abdomen is severe and constant and can last for days. Pain frequently increases when drawing a breath.
2. Pain also may radiate to the back or occur under the shoulder blades.
3. About a third of patients have fever and chills.
4. Nausea and vomiting may occur.
5. Complaints of gas, nausea, and abdominal discomfort after meals are the most common, but they may be vague and indistinguishable from similar complaints in people without gallbladder disease.
6. Jaundice (yellowish skin).
7. Dark urine, lighter stools, or both.

1.1.4 Diagnosis

As majority of patients incur gallstones along with a gall bladder disease, the diagnosis can usually be confirmed thorough ultrasound imaging: a safe, painless and non invasive technique that uses high frequency sound waves to create an image of gallbladder and gallstones. Other diagnosis methods like X-Ray and other scanning technology may be used.

1.1.5 Open Cholecystectomy

In conventional Cholecsytectomy, the surgeon makes an incision approximately 6 inches long. The incision is made either longitudinally in the upper portion of the abdomen or obliquely beneath the ribs on the right side. During some procedure, Drains may be inserted into the abdomen, which is usually removed while the patient is still in the hospital. Following a normal cholecystectomy, the patient may be in the hospital from one to three days following the surgery. Normal activity could be resumed in about four week's time. In complicated cases normal activity could be resumwd in about four to eight weeks. The procedure is very common and is successful most of the time. However, any surgery involves risk factor associated with it, which could cause complications. The most common associated risk with Cholecsytectomy is the injury to the common bile duct (CBD) which is hidden, as it lies below a layer of fat. Thus it is the surgeons expertise and his judgment for the location of CBD and avoiding any injury.

1.1.6 Laparoscopic Cholecystectomy

A laparoscope is a long and rigid tube that is attached to a camera and a light source. Before the laparoscope is inserted, the patient's abdomen is distended with an injection of

carbon dioxide gas, which allows the surgeon to see the internal organs of the patient. With the help of the laparoscope and a video, which guides the surgeon for the procedure, the surgeon will be able to locate and perform cholecystectomy. Other small incisions are made in the abdomen; two of them on the right side below the rib cage and one is in the upper portion below the sternum or the breast. Many other sophisticated instruments are used to perform the procedure. Two instruments are used to grasp and retract the gall bladder and the third one used to free the gall bladder from its attachment. Once the gall bladder is free, the surgeon then removes it out. Under normal conditions, patients would be normal within a day or two. However complications might still occur. The most common complication that could occur is the injury to common bile duct (CBD). This happens in around 0.5% of cholecystectomy. Even though it is rare, it demands a better imaging technique that would provide the surgeon with the precise location of the CBD during cholecystectomy. The imaging technique should also be able to distinguish between the CBD and other tissue, providing a good contrast image.

1.1.7 Current Imaging Techniques

During cholecystectomy, one of the important problems faced by the surgeon is visibility of structures below at layers. Thus it is with the surgeons experience to determine to approximate location of the bile duct. The imaging aid currently available for intraoperative bile duct visualization is intraoperative Cholangiography. This technique has hardly undergone substantial changes since its introduction by Mirizzi in 1937[33]. Routine IOC performed with every cholecystectomy has been determined as one of the strategies to reduce bile duct injuries. The rapidly advancing technology of

nuclear imaging, diagnostic ultrasound, MRI and CT have also been used for the purpose of visualizing the bile duct. Fro diagnosis of hepatobiliary disease imaging techniques such as ultrasound and Magnetic Resonance Cholangiography (MRC) is frequently used. Endoscopic Retrograde Cholangiography (ERC) is one of the standards for visualization of bile duct. Ultrasound is tolerated by patients and is cost effective. MRC is superior in visualizing the biliary system and does not require any contrast agent to visualize the bile ducts and dilatation and gallstones in CBD are easily detected. For patients with choedocholithiasis, Endoscopic retrograde cholangio-pancreatography could be utilized. Selective use of preoperative ERCP has proven to be a good diagnostic tool, as well as a way to allow clearance of CBD stones when present[34]. One of the faster and widely available technique is Computed Tomography Cholangiography (CTC). A multi-detector CT reports a sensitivity of 65%-88% and a specificity of 84%-97% to detect gallstones. With the development of multidetetcor CT, the resolution of CTC exceeds that of MR[35].

1.1.8 Disadvantages of Present Imaging

Even with the use of the above mentioned technology, there are a lot of disadvantages. ERC is an invasive, user-dependent modality which may also induce pancreatitis. Though ultrasound is cost effective, the images are not clearly understood by clinicians. MRC is also often inconclusive in patients with air in the biliary system. Proponents of routine intraoperative cholangiography (IOC) claim that their practice lowers risk of CBD injuries and leads to fewer retained bile duct stones[36] [37]. The disadvantages of routine IOC include increase in costs, operative time and false positive findings, leading to unnecessary efforts to clear the CBD stones. Injecting contrast media

for an CTC can led to adverse effects such as anaphylaxis, urticaria and respiratory distress[35]. These could be reduced if the contrast agents are diffused instead of injecting them. Possible explanations of infrequent use of CTC might be the low resolution of a single detector helical CT and reports of an unacceptable high number of adverse events after the injection of meglumine iotroxate[35]. It has been observed that selective preoperative ERCP was successful in showing CBD stones.

1.2 Fluorescence

Fluorescence is the optical phenomenon of luminescence in which the molecular absorption of a photon triggers the emission of another photon of longer wavelength. The energy difference between the absorbed and the emitted wavelength ends up as molecular vibration or heat. The material that exhibits fluorescence is called a fluorophore. Different fluorophore have different absorption and emission wavelengths. Fluorescence imaging has found a number of applications in the field of Biochemistry and Medicine.

Typically a fluorophore molecule in the ground state, S_o absorbs energy $h\upsilon$ provided by the excitation light. This energy takes the molecule to an excited state S_1. This is an unstable state hence; the molecule returns to the ground state S_o by emitting energy equivalent to $h\upsilon$. Return to the ground state could happen through many paths. This is represented using the Jablonski diagram (Fig 1.2).

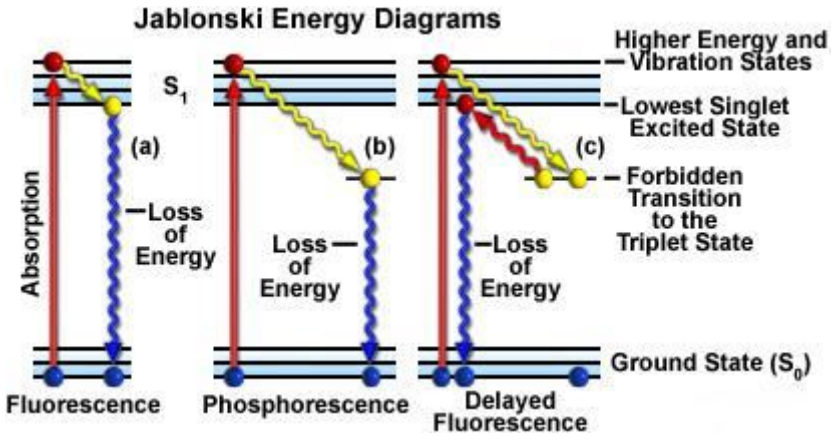

Figure 1.2: Jablonski Energy diagram depicting fluorescence, phosphorescence and delayed fluorescence.

In the current research Indocyanine Green (ICG) and bilirubin are used as fluorophore. ICG has already been established as an injectible fluorophore for retinal angiography. Bilirubin on the other hand exists as a component of bile, thus avoiding injection of a fluorophore.

1.3 Research Problem

One of the major hurdles during cholecystectomy procedure, open or laparoscopic is the visualization of bile duct, which is hidden underneath the fat layers, to avoid any bile duct injuries. As discussed above, any given imaging technique is not fully satisfactory.

The aim of this project is to develop a fluorescence imager that would help us visualize the bile duct either by injection of a fluorophore into the bile duct or by exciting the fluorophore inherently present in the bile duct. This would be accomplished by the use of fluorescence of substances either existing inside the bile duct (bilirubin) or through external injection into the bile duct (Indocyanine Green). A unique design of short pass-

long pass filters would enable us to view all the photons coming out due to fluorescence. The excitation fluorescence filter is coupled to a broadband QTH source, which provides the energy for excitation to the fluorophore. The fluorophore absorbs this energy and emits photons of higher wavelength than the one being absorbed. These photons are detected by the FPA which is coupled to the emission fluorescence filter, designed uniquely to avoid any excitation light. The FPA would produce am image of fluorescence of the fluorophore, which would be used for further analysis and to determine the location of the bile duct.

Thus the goal of this project would be to develop, calibrate and apply this novel fluorescence imager towards visualization of bile duct in-vivo during human cholecystectomy. It is hypothesized that Indocyanine Green could be used as a potential contrast agent to visualize biliary structures using its fluorescence properties.

CHAPTER 2

INSTRUMENTATION

The current study involves a novel fluorescence imagery system for visualizing the biliary tract, in-vivo, using Indocyanine Green and Bilirubin as fluorophore.

2.1 Fluorescence Imager Using ICG

The imaging system consists of a focal plane array sensitive in the near infrared region for imaging Indocyanine green (ICG). The imaging system would help surgeons visualizing the bile duct real-time by exploiting the fluorescence properties of ICG. The imaging system was developed at the Laboratory of Biomedical imaging at University of Texas, Arlington under the politic supervision of Dr. Karel Zuzak.

The system consists of a broadband illumination of light from a 250 W QTH (quartz Tungsten Halogen) lamp placed in housing (Oriel, Stratford, CT). The source is powered by a radiometric power supply to maintain a stable lamp output with minimum light ripple, making it an excellent long term, stable illuminator. The condensing lens assembly contains a molded pyrex aspheric which condenses light to the filters and optical couplers. A liquid light guide (Oriel, Stratford, CT), which also acts as an UV filter that attenuates wavelengths below 420 nm is coupled to the condenser. The other end of liquid light guide is coupled to pyrex aspheric expander which converts a fiber optic light to a collimated light. The broadband illumination is attenuated by a low pass filter mounted in front of this aspheric expander. The low pass filter (Omega Optical,

Brattleboro, VT) was designed taking the ICG absorption characteristics into account. The lowpass filter (LPF) has its cut off (50% Transmittance) wavelength at 795 nm. The detector consists of a high pass filter (HPF) coupled to a 50 mm, f/1.4 lens (NIKON, Tokyo, Japan) which is placed in front of the focal plane array as shown in Fig 2.1

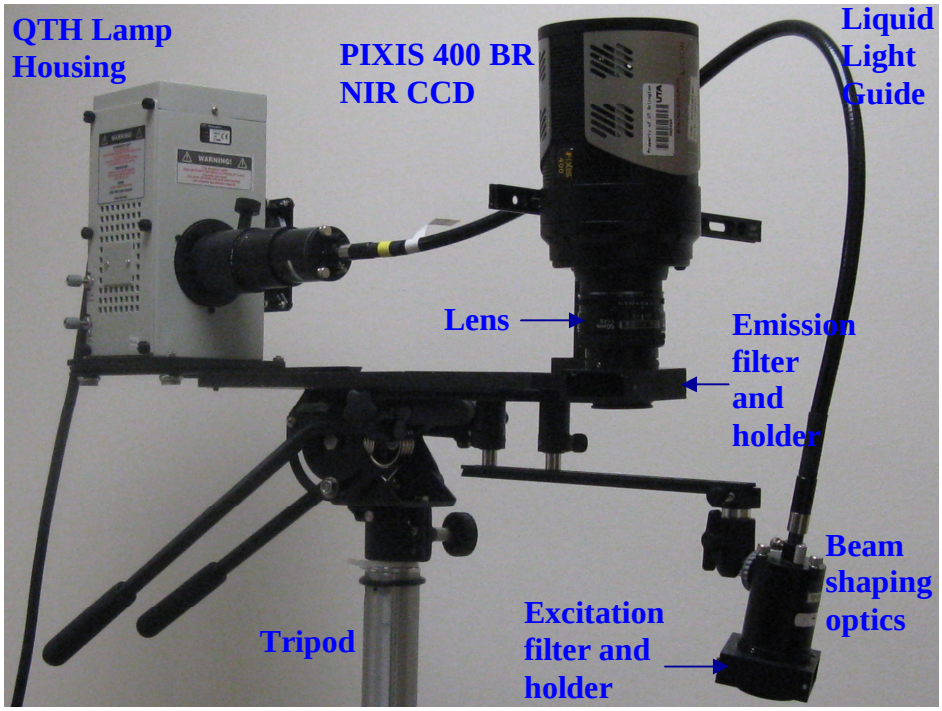

Figure 2.1: Fluorescence Imager for detecting ICG.

The high pass filter (Omega Optical, Brattleboro, VT) has been designed according to ICG emission characteristics. The HPF has its cut off (50% Transmittance) wavelength at 805 nm. The CCD consists of a Focal Plane array. The system utilizes a PIXIS: 400BR (Princeton Instruments, Trenton, NJ). The pixis 400 BR FPA is a fully integrated system with a permanent vacuum/ deep cooling. It uses a high performance, back illuminated, spectroscopic format CCD. The CCD incorporates the deep depletion technology and a proprietary anti-etaloning process to extend the sensitivity in the near

infrared (NIR). These special devices are thermoelectrically cooled (air) down to -75^{o} C to provide the lowest dark charge, hence reduction of dark current noise. The FPA has a 1340 x 400 array with 8mm chip height and 27 mm spectral coverage. This makes the FPA ideal for multistripe spectroscopy and maximum light collecting area. Each pixel has a size of 20 μm x 20 μm with an imaging area of 26.8mm x 8.0 mm. The sensitivity ranges from 220 nm to 1100nm, with a peak efficiency of about 85% at ~ 800nm. The pixis has a 16 bit Analog to Digital Converter (ADC) coupled to the FPA, thus giving a maximum of 2^{16} (655356) shades of gray[8]. A high end laptop (Dell Latitude D610: Austin, Texas) is connected to the camera for image rendering and analysis. The system specified above would be helpful for the surgeon to visualize the common bile dust during cholecystectomy.

2.2 Fluorescence Imager Using Bilirubin

The fluorescence imaging system using bilirubin as a fluorophore consists of a Focal Plane Array which is sensitive in the visible region. The system consists of a broadband illumination of light from a 250 W QTH (quartz Tungsten Halogen) lamp placed in a housing (Oriel, Stratford, CT). The source is powered by a radiometric power supply to maintain a stable lamp output with minimum light ripple, making it an excellent long term, stable illuminator. The condensing lens assembly contains a molded pyrex aspheric which condenses light to the filters and optical couplers. A liquid light guide (Oriel, Stratford, CT), which also acts as an UV filter that attenuates wavelengths below 420 nm is coupled to the condenser. The other end of the Liquid light guide is connected to a beam expander/collimator. A low pass filter (Omega Optical, Brattleboro, VT) with a cut off (50% Transmission) at 500nm, designed on the basis of absorption properties of

bilirubin is coupled to the collimating assembly. A high pass filter (Omega Optical, Brattleboro, VT) with a cut off (50% Transmission) at 515 nm, designed on the basis of emission properties of bilirubin is coupled to a 50 mm, f/1.4 lens (NIKON, Tokyo, Japan) which is placed in front of the focal plane array as shown in Fig 2.2.

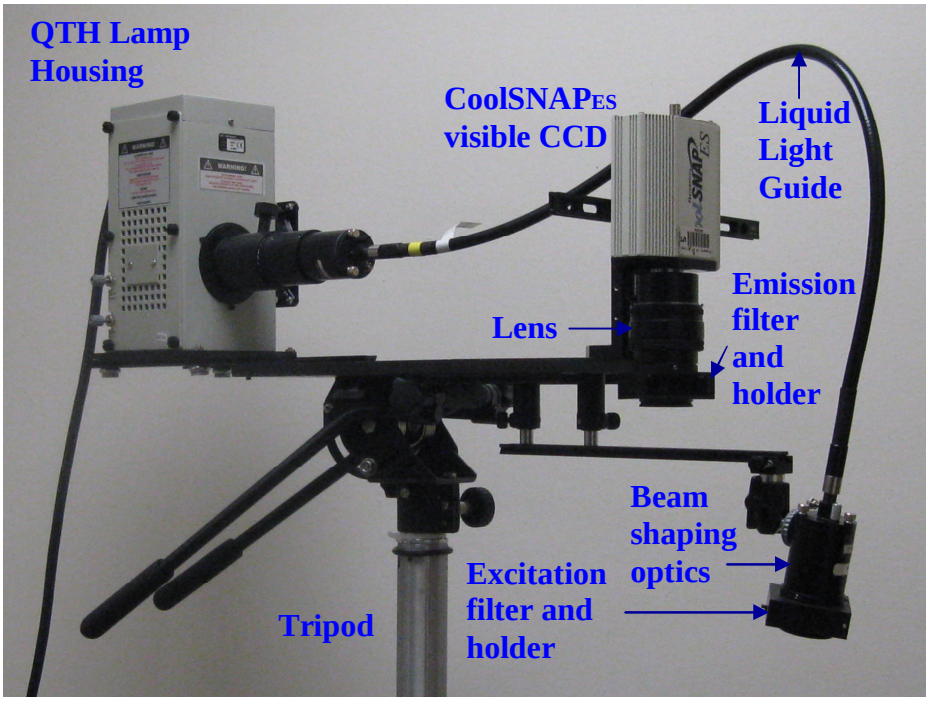

Figure 2-2: Fluorescence Imager for Bilirubin

The UT, Arlington fluorescence system uses CoolSnap$_{ES}$ (Photometrics, Tucson, AZ) contains a Sony ICX 285 focal plane array. Higher sensitivity is one of the distinct advantages of this CCD which enables it to have reduction in time for data collection. The analog to digital converter (ADC) is 12 bits with a speed of 20Mpixels/s, decreasing the acquisition time by a factor of 20 when digitizing the same number of pixels.

2.3 Components of the System

2.3.1 Quartz Tungsten Halogen (QTH) Lamp & Radiometric power supply

The QTH source (Lamp and Housing) along with the radiometric power supply is shown in Fig 2.3 below. The QTH source and power supply are manufactured by Spectra- Physics, a division of Newport Corporation.

Figure 2.3:(A) Research Grade lamp housing (Model: 66884). (B) Radiometric Power Supply (Model: 69931)

The research Grade lamp housing (Model: 66884) houses a 250 W QTH lamp source (Model: 6334) as shown in the Fig 2.3 (A) and the Radiometric power supply (Model: 69931) drives the source. Fig 2.3 (B).

The Oriel Radiometric Power Supply is a highly regulated source of constant current or constant power for Quartz tungsten halogen lamps. The control and monitoring features of the power supply include powering the supply on and off, set the

current/power preset and limit, monitor the current, voltage, power and operating time. The power supply is run in current mode with a current setting at 10.42 Amps, which drives the QTH lamp[11]. The Research grade lamp housing holds the QTH lamp. The housing includes condensing optics to produce a collimated or focused beam. Asphere condensers are used for superior uniformity. The housing also incorporates rear reflectors to collect the lamp's back radiation, external lamp and reflector adjustments to fine position the filament and a power regulated fan to cool the lamp and the housing[10]. Re-imaging onto the filament does increase the collimated output a little and changes the power balance of the system.

Table 2-1: Specification of Radiometric Power Supply (Model 69931)

Parameters	**Model 69931**
Power Factor	>0.99
Input Voltage	90 - 264 VAC
Input Current	5 A
Input Frequency	47 - 63 Hz
Output Power	40 - 300 W
Output Current	3 - 24 A
Output Voltage Range	0 - 45 VDC
Line Regulation	0.01 %
Output Voltage Ripple	<0.05 % r.m.s.
Light Ripple	<0.05 % r.m.s.
Meter Accuracy (% of full scale)	<0.05 %
Digital Meter Resolution, Voltage	0.1 VDC
Digital Meter Resolution, Current	0.01 A
Digital Meter Resolution, Power	1 W
Safety Interlock Voltage	12 VDC/GND
Operating Mode	Constant current or constant power
Ambient Operating Temperature	0 - 45 °C
Weight	20 (9)
Dimensions (W x D x H) [in. (mm)]	12.0 x 16.0 x 5.18 (305 x 406 x 132)

Quartz Tungsten Halogen lamps are popular visible and near infrared sources because of their smooth spectral curve and stable output. They do not have sharp spectral peaks that arc lamps exhibit and they emit little UV radiation as depicted in the Fig 2.4 below[12].

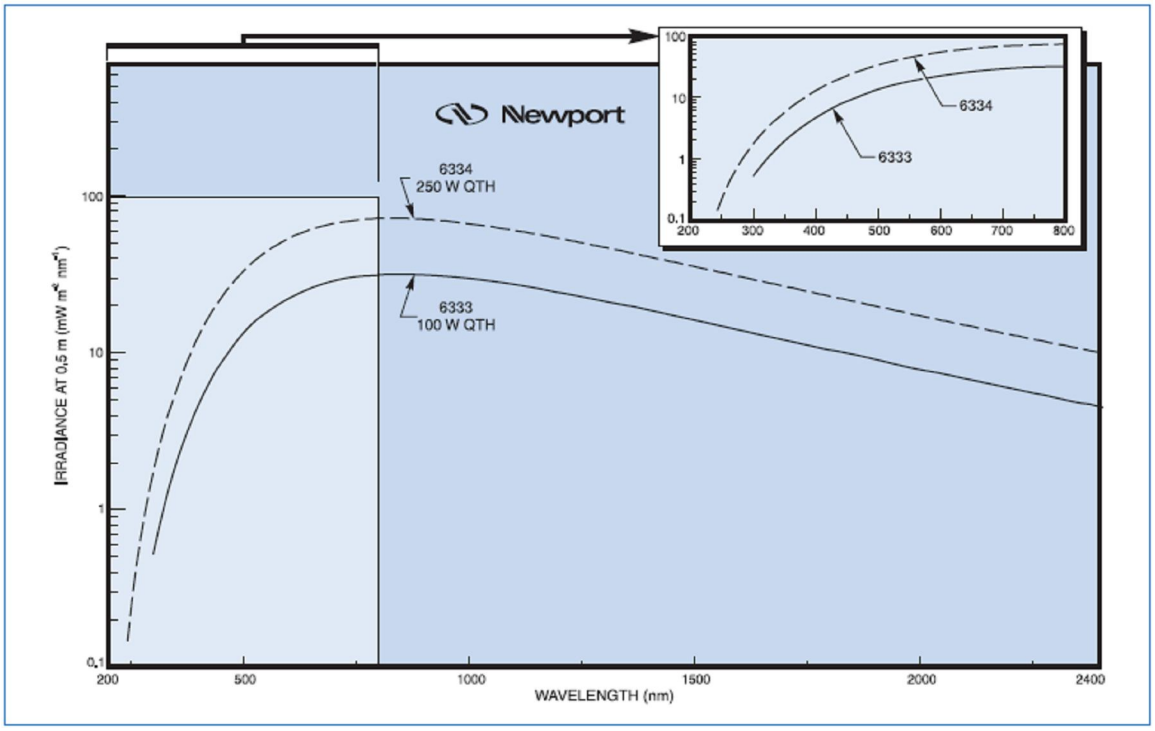

Figure 2.4: Spectral Irradiance at 0.5m of 100 W (6333) and a 250 W (6334) QTH lamp[13]

2.3.2. Filters

Indocyanine Green (ICG):

ICG has a molecular formula of $C_{43}H_{47}N_2NaO_6S_2$. The filter designs have to be designed based on the emission and absorption spectrum of ICG. ICG has a bimodal absorption spectrum from 650 nm- 800 nm with peaks occurring at 685 nm and 775 nm in distilled water. In plasma, ICG has two absorption peaks at around 710 nm and 805 nm. The absorption spectrum changes according to the concentration of ICG and solvent. Higher

concentration has its maximum absorption at 685 nm while lower concentration has its maximum absorption at 775 nm in aqueous solution[15]. Thus separate filters were designed for ICG with water as a solvent and ICG with blood as a solvent. A unique filter design was developed at the Laboratory of Biomedical Imaging at UT Arlington. Instead of a conventional Band pass filter combination for emission and excitation filters a unique low pass and high pass filters were used as Excitation and Emission filter.

As discussed before, the excitation filter were designed according to ICG absorption characteristics, This is depicted in fig 2.5, where the dashes line displays the absorption spectrum of ICG in distilled water with a concentration of 0.015 mg/ml.

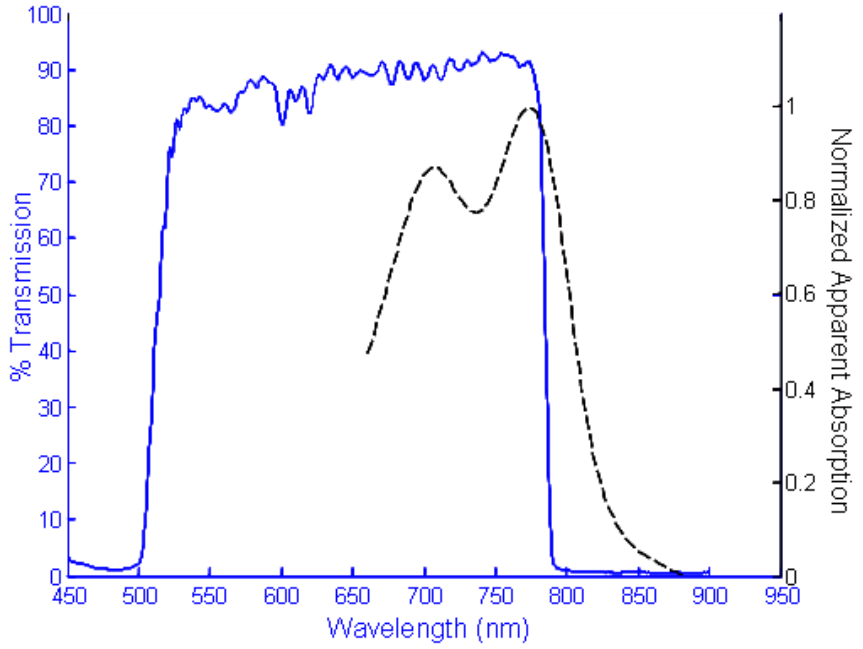

Figure 2-5: Excitation Filter Transmission characteristics for ICG in distilled water (Blue). The Black curve depicts the absorption spectrum of ICG in distilled water having a concentration of 0.015 mg.ml

ICG in Distilled Water:

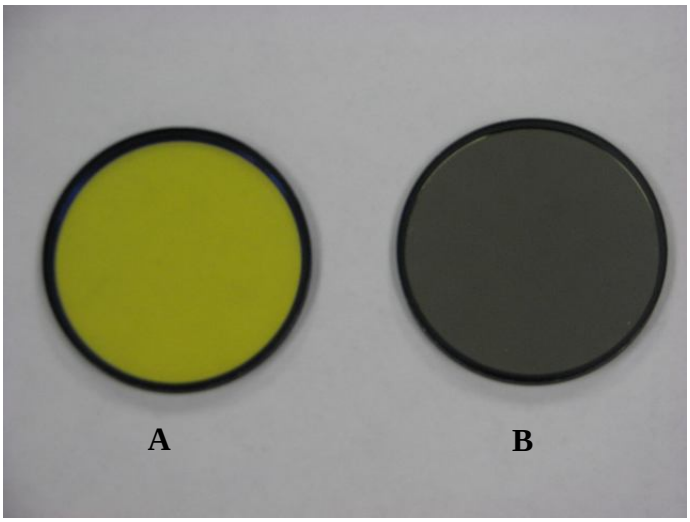

Figure 2.6: (A) Excitation Filter for ICG in Aqueous solution. (B) Emission Filter for ICG in Aqueous Solution.

The filter combination (Excitation and Emission) of low pass and high pass were used. The low pass filter had a cut off (50% Transmission) wavelength at 790 nm. This filter coupled with the source (mentioned above) would be used to excite ICG with all possible absorption wavelengths of ICG including peak absorption wavelength. The high pass filter (coupled with the detector) were used to collect the fluorescence photons coming from ICG. In aqueous solution ICG has an emission peak at 820 nm[16]. Thus a high pass emission filter with a cut-off (50% Transmission) at 805 nm is used. This enables us to avoid any excitation light reflected back. The excitation and emission filter characteristics are shown in the Fig 2.9 and Fig 2.10 respectively. These curves were obtained by using a standard calibrated USB2000+ spectrometer (Ocean Optics, Dunedin, FL) and using the filter in the transmission mode and illuminating with a broad band source, discussed above.

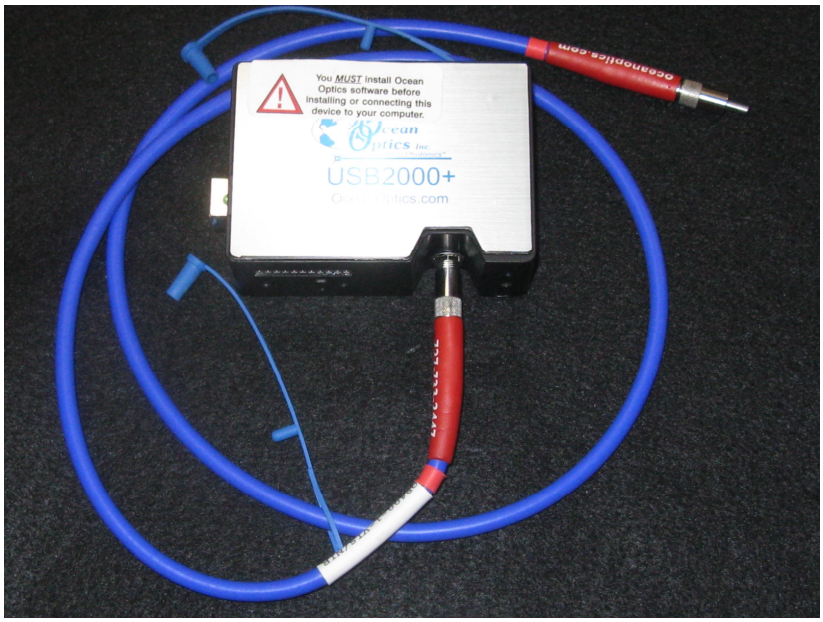

Figure 2.7: USB 2000+ Spectrometer (Ocean Optics, Dunedin, FL)

During the entire experiment all the parameters including distance, exposure time and other pre processing remained the same.

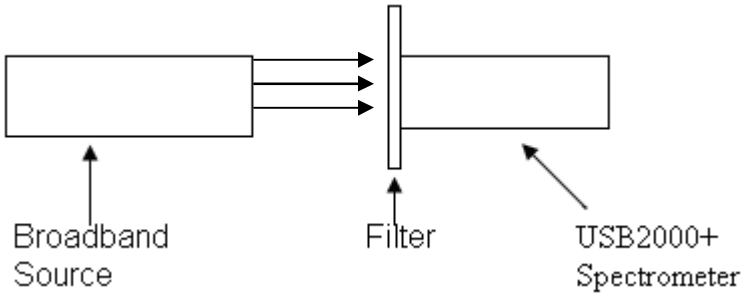

Figure 2.8: Set up for measuring the Excitation and Emission Filter characteristics. This set up was used for finding the transmission curve of all filters.

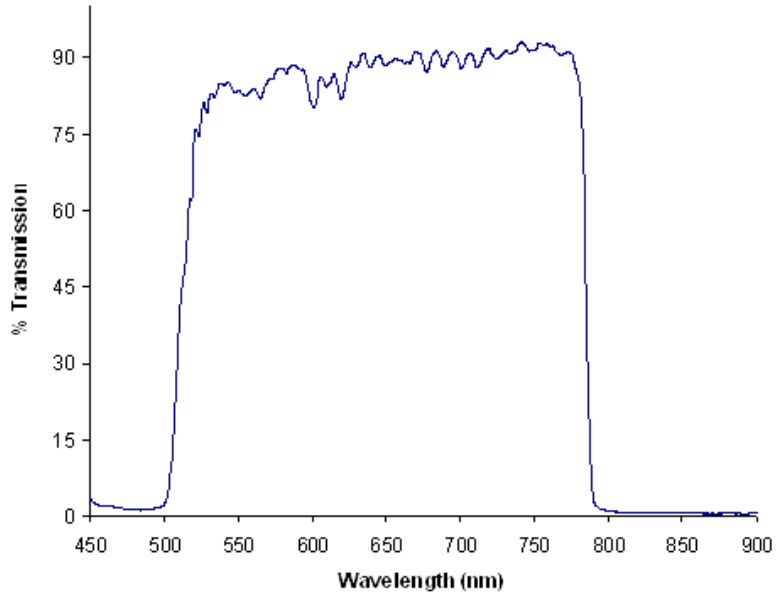

Figure 2.9: Short pass filter transmission characteristics used as an excitation filter for ICG in aqueous solution.

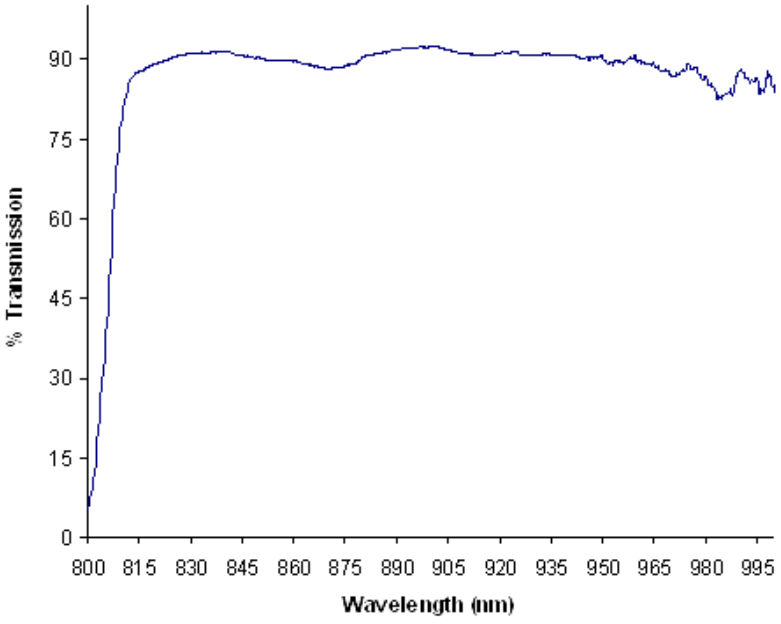

Figure 2.10: Long pass filter transmission characteristics used as an emission filter for ICG in aqueous solution.

ICG in Blood:

The design follows a similar pattern as that for ICG in aqueous solution with changes in the Excitation and Emission cut-off filters. The low pass excitation filter has a wavelength cut off (50% Transmission) at 810 nm. This filter coupled with the source would enable us to illuminate the target (ICG) with its entire absorption wavelength. ICG emission occurs at 830 nm when in blood[16][17]. Thus the high pass emission filter has a filter cut-off (50% Transmission) at 815 nm allowing us to view only the fluorescence photons coming into the detector. The excitation and emission filter transmission characteristics are shown in fig 2.11 and fig 2.12.

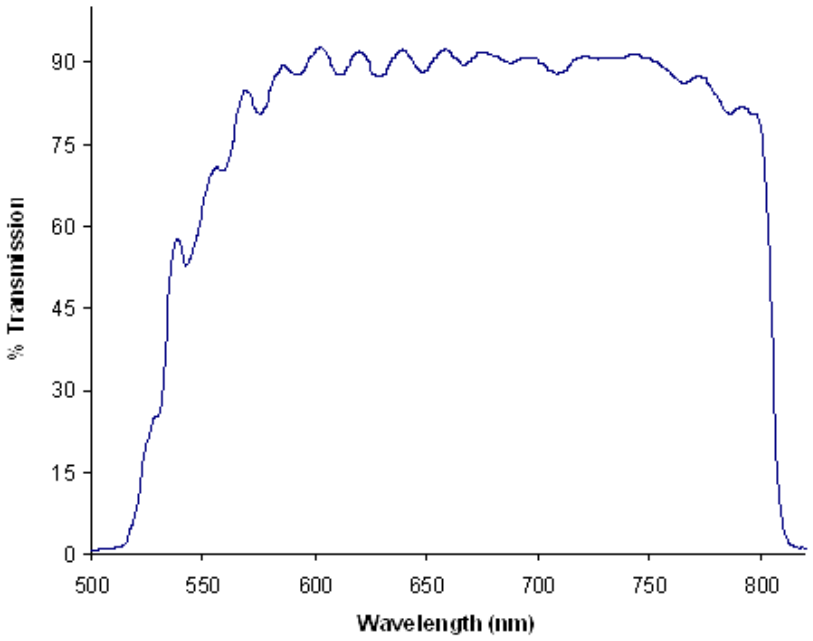

Figure 2.11: Short pass filter Transmission characteristics used as an excitation filter for ICG in Blood.

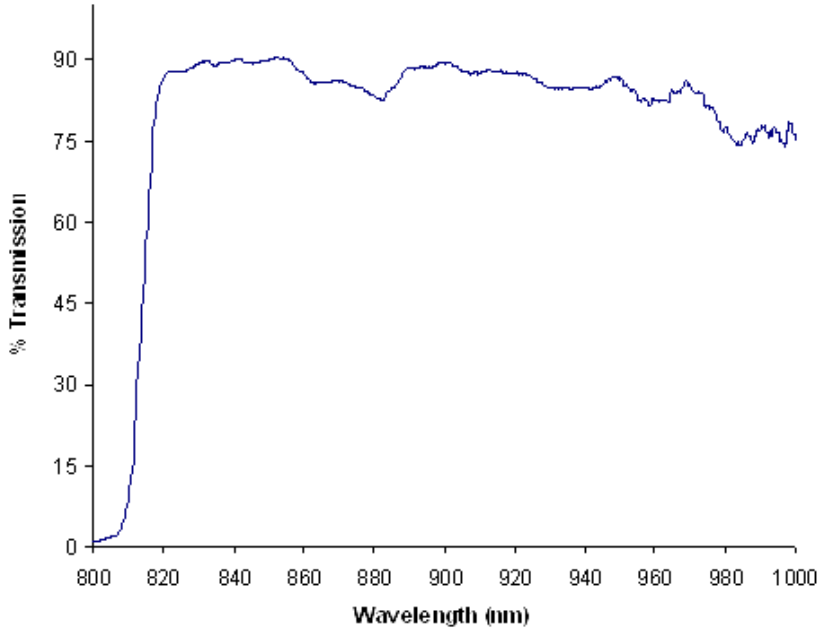

Figure 2.12: Long pass filter Transmission characteristics used as an excitation filter for ICG in Blood.

*Bilirubin***:**

Bilirubin stands as one of the important constituents of bile. The pH of bile ranges fomr 7.5- 9.5, which shows that bile is alkaline. This is due to the presence of bicarbonates. Bilirubin is a major product of heme catabolism. Bilirubin is a yellow tetrapyrrole pigment which is water soluble as it possesses two propionic side chains, which might be expected to render it highly polar. But bilirubin could be water insoluble as the bilirubin molecule can adapt to various configurations. Bilirubin is mostly found in the conjugated form in bile. Unconjugated bilirubin is normally 5% of total bilirubin. Bilirubins are also susceptible to oxidation and are photosensitive, thus leading to a variety of derivatives[31]. The quantum yield of free bilirubin at room temperature is low ($< 10^{-4}$). [18] Thus fluorescence of free bilirubin is difficult to observe. However fluorescence of bilirubin is enhanced in the presence of Albumin[32].

Bilirubin in bile fluoresces as a result of its interactions with other bile components and albumin. Thus imaging this fluorescence would be an indicator for the position of bile duct, which contains bile in it. Bilirubin has a strong absorption of visible light between 400 nm -500 nm[31]. Thus a filter designed to allow ideally all the wavelengths below 500nm would become an excellent excitation filter for fluorescence of bilirubin in bile. This was the basis of the excitation filter design. The transmission characteristics of such a filter is shown below in fig 2.13 and fig 2.14

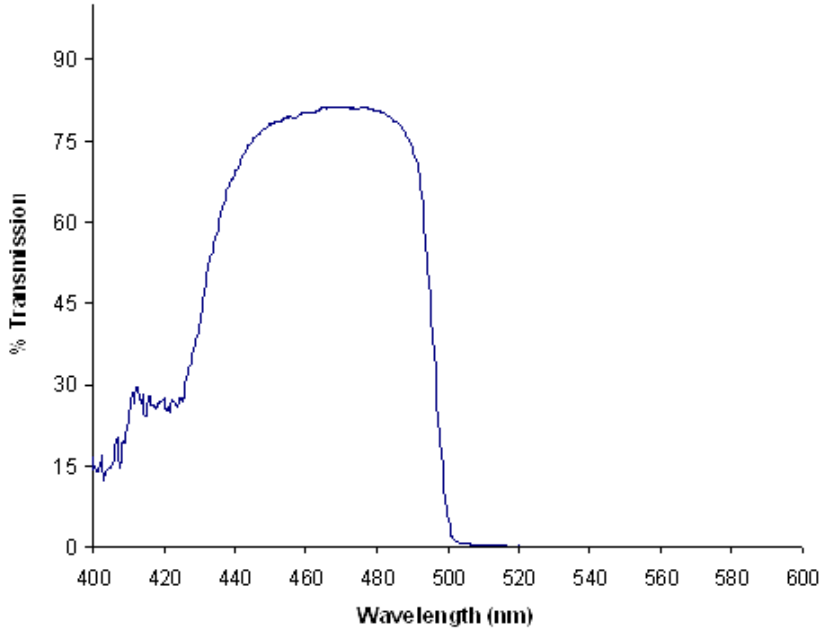

Figure 2.13: Short pass filter Transmission characteristics used as an excitation filter for Bilirubin.

The fluorescence of bilirubin in bile is observed to peak around 528 nm[32]. Thus a filter capable of eliminating the excitation wavelengths and able to measure or see the fluorescence was designed. Such a design was implemented through a long pass filter with its cut off (50%) at 515 nm. The transmission is shown in fig below.

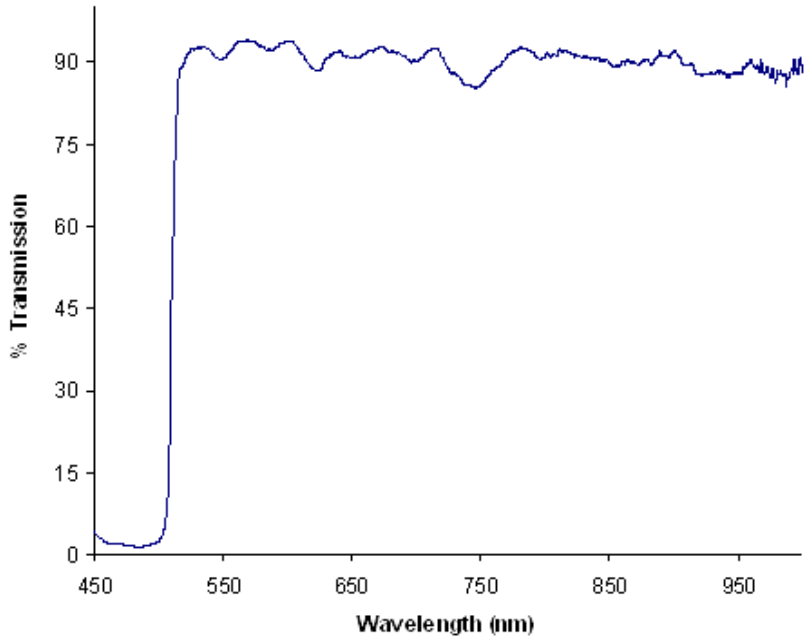

Figure 2.14: Long pass filter Transmission characteristics used as an excitation filter for Bilirubin.

2.3.3 Camera Lens

Figure 2.15: 50 mm/ F 1.4 Nikorr Lens

The Emission filter is coupled to a 50 mm/ F1.4 Nikorr Lens manufactured by Nikon as shown in the fig 2.15 above. This helps in focusing the target onto the CCD. This lens is fast enough for shooting just about any type of light. It produces distortion free images with high resolution and color rendition. This makes it an ideal lens perfect for any type of light shooting. This lens incorporates a wide variety of f-stop or aperture. The maximum aperture is f/1.4 while the minimum aperture is f/16[19]. The back end of the lens is coupled to a C-F mount, which is used to fit a variety of lenses onto the CCD.

2.3.4 Focal Plane Array

The Charged Coupled Device or Focal Plane Array is an analog shift register that enables analog signals to be transported through successive stages controlled by a clock signal. An image is projected by a lens onto the photoactive region of the CCD which consists of photodiodes and capacitors that accumulate charges based on the intensity of light at that location. This image is then transferred to the transmission region, which consists of shift registers. Once the array has been exposed to the image, a control circuit causes each capacitor to transfer its content to its neighbor. The last capacitor dumps the charge to a charge amplifier, which converts the charge into a voltage and is finally read out[20].

PIXIS 400 BR:

The Focal Plane Array used for imaging Indocyanine Green (ICG) is the Pixis 400 BR as shown in Fig 2.16.

Figure 2.16: Pixis 400BR Focal Plane Array

The specifications for Pixis 400BR is given in the table below.

Table 2-2: Specification for PIXIS 400 BR

CCD Format	1340 x 400 imaging pixels 20 x 20-µm pixels 100% fill factor 26.8 x 8.0-mm imaging area
System Read Noise	5 e-rms @ 100-kHz digitzation (max) 16 e-rms @ 2 MHz digitization (max)
Spectrometric Well Capacity	300 ke- (High Sensitivity- Typical) 1 Me- (High Capacity- Typical)
Deepest Cooling Temperature	-70^{o}C (High Sensitivity) Minimum -75^{o}C (High Sensitivity) Typical
Dark Current @ -75oC	0.25 e-/p/s (Typical) High Sensitivity 0.5 e-/p/s (Maximum)
Dynamic Range	16 Bits
Vertical Shift Rate	30 µsec per row
Operating Environment	+5 to +30^{o}C non-condensing

PIXIS 400 BR has controlling software that controls and maintains the set temperature allowing a deviation of ± 0.05^{o}C from the set temperature by controlling the camera's cooling circuit. Dark charge is thermally induced into the FPA over time. This statistical noise is called the Dark Noise. Dark noise tends to change depending on the exposure time, temperature and gain. Dark noise could be measured when there is no light passing through the FPA. The longer the exposure time and warmer the temperature, the background would be larger and less uniform[21]. The camera has controller gain

software which allows us to set three different gain levels. Level 1(low) is used for high signal intensities. Level 2(mid) is used for mid intensity levels and Level 3 (High) is used for low intensities.

From the specification table one could see that the camera has a dual digitization rate available (100 KHz/ 2 MHz). The 2 MHz digitization rate is used for fastest possible data collection while the 100 KHz would be used when noise performance is of greatest concern. Thus Multi digitization allows complete freedom between 'Slow Operation' for low noise and high SNR and 'Fast Operation' for rapid spectral acquisition[21][22][8]. Megapixel resolution and smaller pixel size allows imaging very fine details. Sensitivity can be improved by binning, but at the expense of resolution. The camera has a 1340 x 400 CCD array that provides superior resolution over industry standard '1024' pixel format. Binning increases the frame rate. The camera has a dynamic range of 16 bits allowing bright and dim signals to be quantified in a single image with 2^{16} shades of gray [8].

The quantum efficiency curve of PIXIS 400 BR is shown in fig 2.17. PIXIS 400 BR had a back illuminated FPA. This means that light enters from back surface through thinned (Etched) silicon layer. This has an advantage that no light absorption and reflection takes place at the polysilicon gate structure enabling the CCD to have higher quantum efficiency (almost twice)[23]. Due to this etching, the layer becomes transparent to NIR wavelength causing fringe effects for NIR spectroscopy. To overcome the disadvantages of etaloning the CCD is made of thicker silicon (roughly twice the thickness of a normal back-illuminated CCD). This contributes significantly for the absorption of NIR light,

reducing the amount of light that survives a round trip path to cause interference and increasing the quantum efficiency[23].

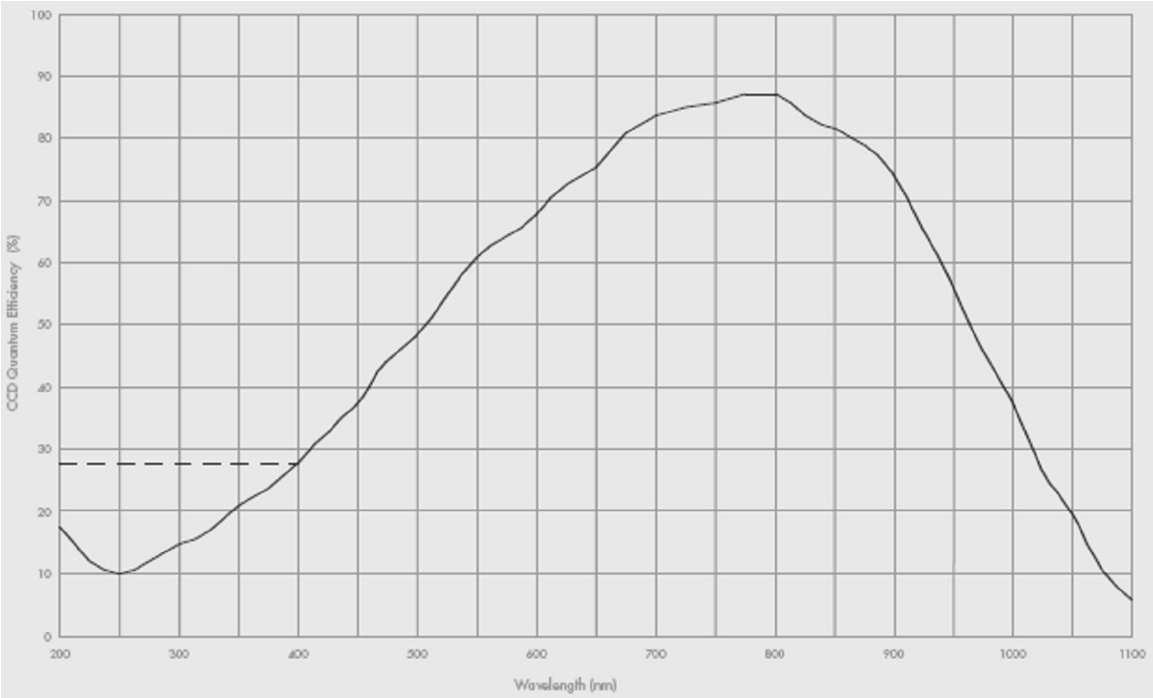

Figure 2.17: Quantum Efficiency Curve for PIXIS 400 BR. [8]

The back surface is typically AR coated, which is optimized for NIR wavelengths. This reduces the amount of light into the CCD that is reflected back from the polysilicon side of the back surface. It also increases the quantum efficiency by increasing the amount of light into the CCD and reducing stray light in the spectrometer.

COOLSNAP$_{ES}$

Figure 2.18: CoolSNAP$_{ES}$ FPA detector used for imaging bilirubin

The CoolSnap$_{ES}$ camera is used as a detector for measuring the fluorescence of bilirubin. This camera has high quantum efficiency in the visible region which makes it a perfect choice for fluorescence measure of bilirubin. This camera is used in applications requiring high speed and high spatial resolution in the visible region. It is manufactured by Roper Scientific (Now Princeton Instruments). The CoolSnap$_{ES}$ offers higher sensitivity and lower read noise to produce high quality 12-bit monochrome images[25].

The specification table is provided below:

Table 2-3: Specifications of CoolSnap$_{ES}$ FPA

Specification CoolSnap$_{ES}$	
CCD Format	1392 x 1040 imaging pixels 6.45 x 6.45-µm pixels 8.77 x 6.6-mm imaging area (Optically Centered)
System Read Noise	< 8 e-rms @ 20MHz
Well Capacity	16000 e- (Single Pixel) 30000 e- (2 x 2 Binned Pixel)
Cooling	Thermoelectric, 5oC below ambient Temperature
Dark Current	1 e-/p/s
Dynamic Range	12 Bits @ 20MHz
Dimensions	4.5" x 5.0" x 2.5" (1.9 lbs)
Operating Environment	15^{o}C to 30^{o}C ambient
Frame readout	91 ms/frame

The CoolSnap$_{ES}$ incorporates a SONY ICX285AL silicon chip array with interline transfer capability. The interline-transfer CCD has a parallel register that is subdivided into alternate columns of sensor and storage areas. The image accumulates in the exposed area of the parallel register and during CCD readout the entire image is shifted under interline-mask into a hidden shift register and then proceeds in normal CCD fashion. Since the signal is transferred in microseconds, smearing is undetectable for typical

exposures. However, a drawback to interline-transfer CCD's has been their relatively poor sensitivity to photons since a large portion of each pixel is covered by the opaque mask. As a way to increase the detectors fill factor, high quality interline-transfer devices have microlenses that direct the light from a larger area down to the photodiode[24].

The spectral response of $CoolSnap_{ES}$ is shown in the fig 2.19 below

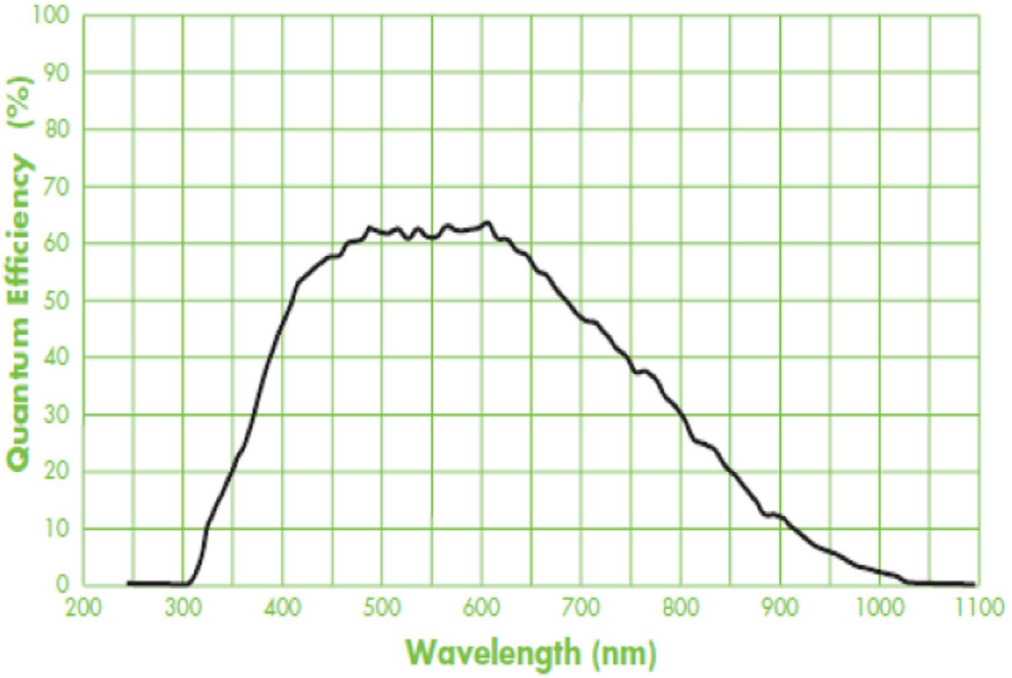

Figure 2.19: Quantum Efficiency of $CoolSnap_{ES}$

From Fig 2.19 above we can clearly see that the quantum efficiency is about 60 % in the region of bilirubin-albumin fluorescence (500nm -550nm), hence used as a detector for measuring fluorescence of bilirubin-albumin.

Both the above mentioned detectors are driven by Photometrics Virtual Camera Access Method (PVCAM) software. The PVCAM application programming interface for high-performance digital cameras is a set of software library routines that implements a camera's operations in a hardware-independent, platform independent suite of function

calls[26]. This software is used to control and acquire data from the camera. The data collection is done using Vpascal programming integrated in V++ which internally communicates with PVCAM for controlling the detectors.

Binning:

Binning is a process of combining charge from adjacent pixels in a CCD during readout. This process is performed prior to digitization in the on-chip circuitry of the CCD by specialized control of the serial and parallel registers. The two primary benefits of binning are improved signal-to-noise ratio (SNR) and the ability to increase frame rate, at the expense of spatial resolution. Binning 1 x 1 has the maximal spatial resolution. No charges are combined in this case. In the case of 2 x 2 binning, during parallel readout, the charges from two rows of pixels, rather than a single row, is shifted into the serial register. Next, charge is shifted from the serial register, two pixels at a time, into the summing well. It the goes to the out put amplifier. This process is iterated until the entire array is read[27].

One of the prime advantages of binning is high SNR. In normal operation CCD read noise will be added to each pixel whereas during binning the CCD read noise is added to each super pixel, thus increasing the SNR. A 2 x 2 binning process is shown in the fig 2.20 below.

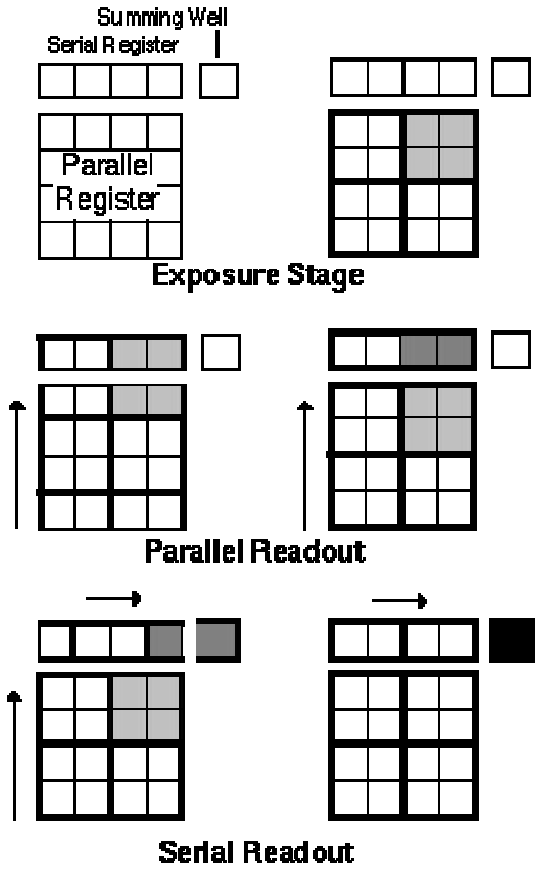

Figure 2.20: 2 x 2 binning process.

CHAPTER 3

INDOCYANINE GREEN FLUORESCENCE IMAGER: CHARACTERIZATION

Indocyanine Green (ICG) ($C_{43}H_{47}N_2O_6S_2Na$), molecular weight of 775, is a trycarbocyanine type of dye with infrared absorbing properties. ICG has little or no absorption in the visible region[29]. The molecular structure of ICG is shown in the fig 3.1 below,

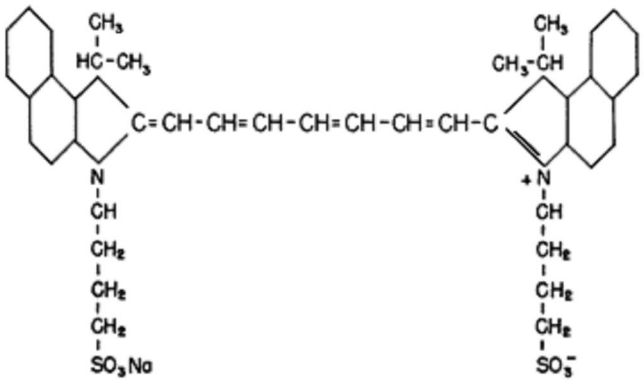

Figure 3.1: Molecular structure of Indocyanine Green (ICG) [30]

After its introduction by Fox et. al. ICG soon came into general use for recording dye dilution curves, in particular for determination of cardiac output. The principle paramount advantage of using ICG as a dye is its absorption maximum at isobestic point of hemoglobin and oxy-hemoglobin, the confinement to vascular compartment through plasma protein binding, low toxicity and rapid excretion into the bile[15]. ICG is readily soluble in water. Following intravenous injection ICG binds to plasma proteins with

albumin as its principle carrier. ICG undergoes no significant extra hepatic or entero hepatic circulation. ICG is taken up by plasma almost exclusively by the hepatic parenchymal cells and is rapidly excreted into the bile. Due to its properties ICG is used extensively for the study of hepatic function[29]. ICG is FDA approved and could be used with proper dosages as per regulation of FDA. IC-Green™ is available in vials from Akorn Inc. Dosages for ICG could also be taken form the same.

It has been demonstrated that ICG could be used as a contrast agent in animals for visualizing biliary tract during Laparoscopic Cholecystectomy[38][39]. This, however does not exploit the fluorescence properties of ICG for the purpose. Thus the proposed method exploits the fluorescence properties of ICG for viewing the biliary tract during cholecystectomy.

3.1 Percent Contrast and Spatial Resolution

The spatial resolution of the fluorescence imager was established by computing the percent contrast by imaging a standard USAF 1951 resolution target. The block diagram for the set up is given in fig 3.2. The distance between the source and the target was set as 22”. The results are plotted for multiple bins.

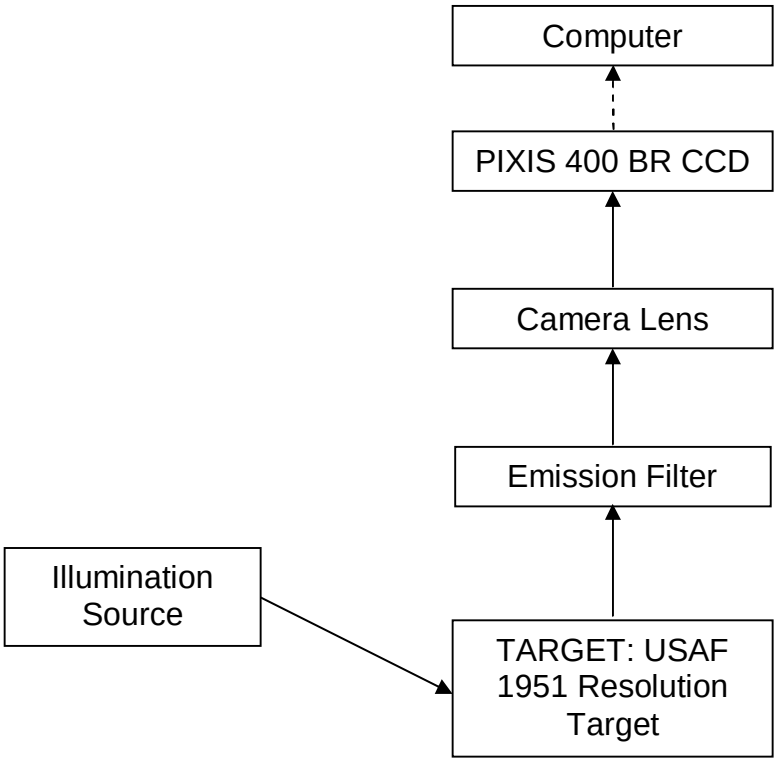

Figure 3.2: Block diagram depicting the method for computing the spatial resolution of the system**.**

Results:

The plot for percent contrast against spatial resolution is depicted in fig 3.3. The percent contrast,C, where I_{max}, maximum intensity reflected by a line of the resolution target (White Bar) and I_{min}, minimum intensity from the non reflecting area between the white bars (Dark bars).

Percent Contrast Calculation:

Percent contrast was calculated by using the equation

$C = (I_{max} - I_{min} / I_{max} + I_{min})$

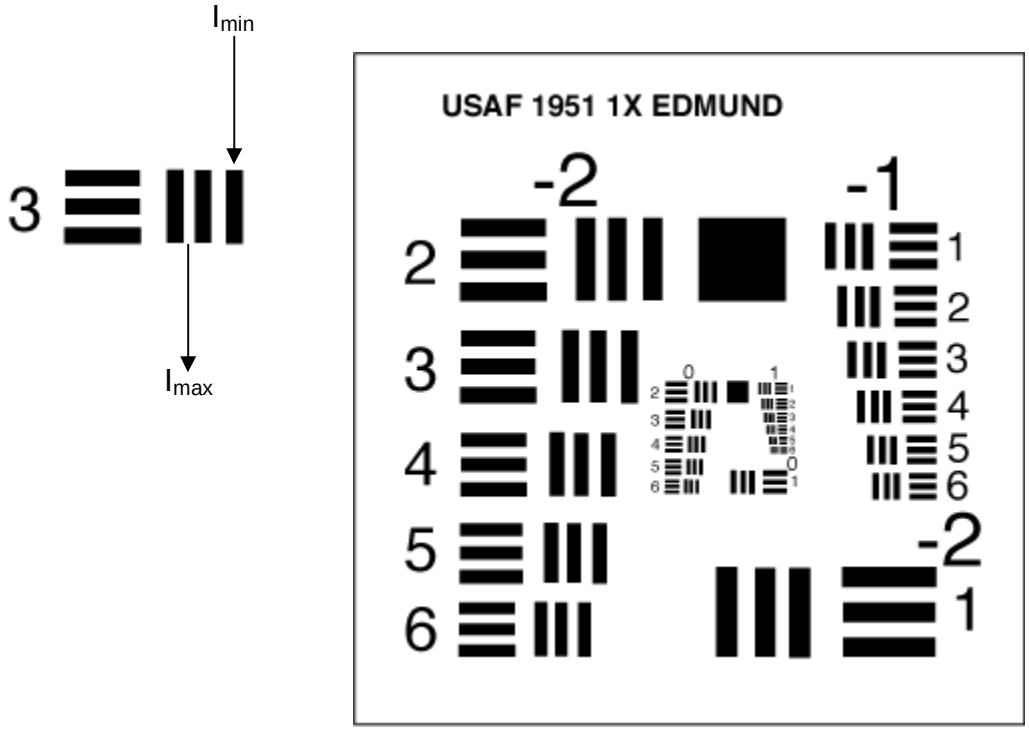

Figure 3.3: Standard USAF Resolution target and Computation of Percent Contrast.

This percent contrast measurement was carried out wuth and without the emission filter on the detector end, to figure out any effects on spatial resolution due to the filter.

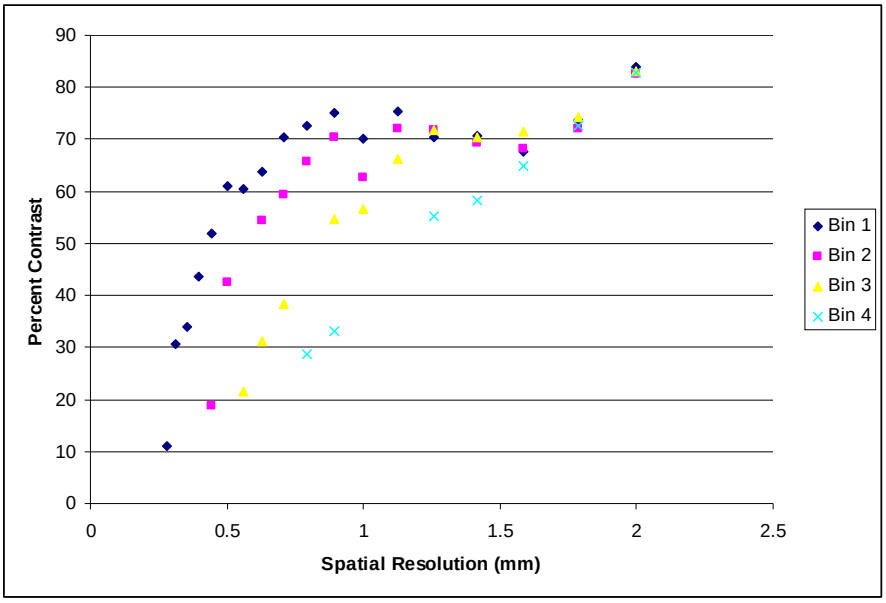

(A)

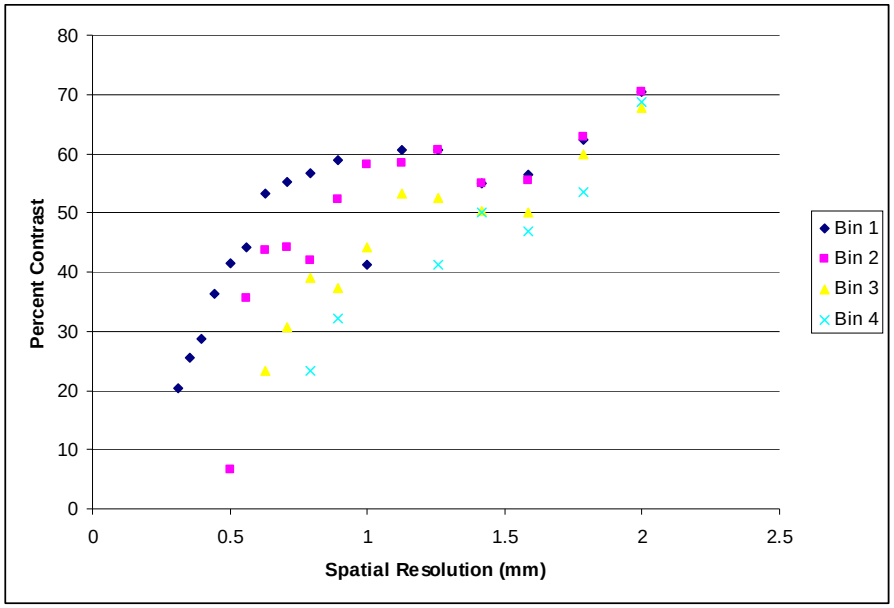

(B)

Figure 3.4: Percent contrast against spatial resolution. (A) Without Emission filter at the detector (B) With Emission Filter at the detector

From the plots of fig 3.4, there is a slight reduction in percent contrast when the emission filter is placed in the path. This could be attributed to the way the filters are manufactured. The surface of the filters is not always smooth and hence there could be a reduction in the spatial resolution. With the filter in place the spatial resolution of the system (Not for fluorescence) turns out to be 0.4mm when used with lowest bin (Bin 1).

3.2 Absorption Spectrum of ICG

The first step in determination of ICG as a potential fluorophore for visualizing biliary tract during Cholecystectomy was to find its absorption spectrums and wavelengths needed for ICG to get excited for fluorescence. ICG has a bimodal absorption peak when in aqueous solution (Distilled Water). The absorption spectrum changes with different solutes of ICG and different concentration. This observation leads to the conclusion that ICG does not obey Beer Lamberts law. There is however a low concentration region where it does obey Beer Lamberts law[15].

Method:

The set up for measuring the absorption spectrum of ICG is shown in the Fig 3.5.

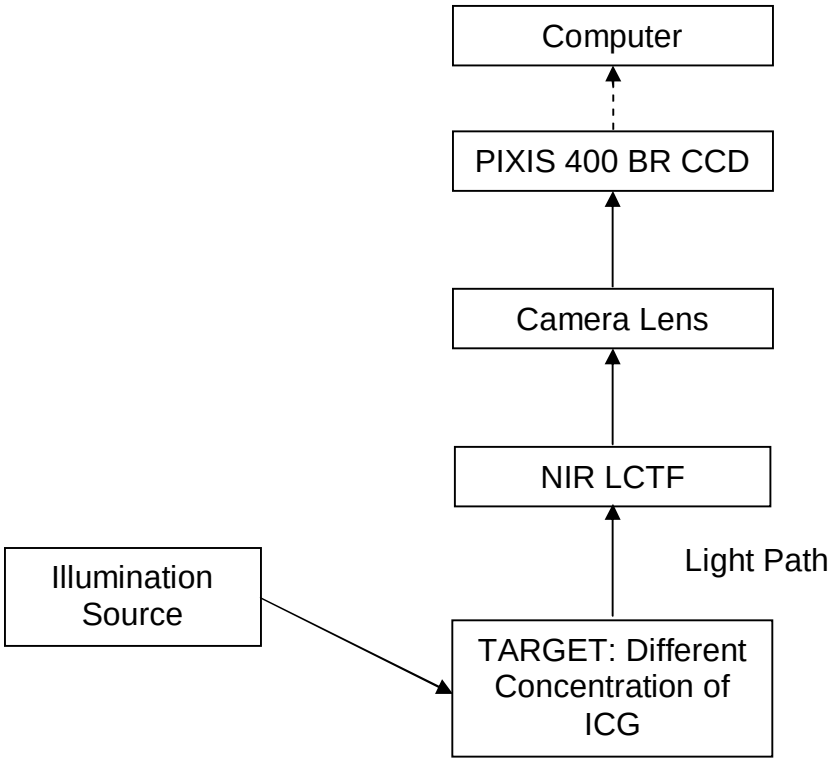

Figure 3.5: Block diagram depicting the set up used for measurement of absorption spectrum of ICG

A QTH lamp, as discussed above, along with all its optical components is coupled to a low pass filter (Excitation Filter: Cutoff 790 nm), which acts as an excitation filter for the fluorophore ICG. Cardio Green (Sigma Aldrich, St. Louis, MO) was used. Three different concentration of ICG (0.078 mg/ml, 0.015 mg/ml and 0.005 mg/ml) were prepared. An initial solution of 0.078mg/ml was prepared and all the other concentrations were obtained by dilution of this one. Thus any error in the measurement of ICG would be consistent. These were filled inside capillaries of 1.5 mm bore diameter. The detector (PIXIS 400 BR) is coupled to a NIR Liquid Crystal Tunable Filter (LCTF) (Cambridge Research & Instrumentation, Boston, MA) which is already calibrated. The distance between the source and the target was set to 22” for all the concentrations. It is possible

to tune the LCTF for different wavelengths and get images at each of those wavelengths. The wavelengths and interval between wavelengths is user defined through software. In this case the LCTF was tuned for wavelengths from 650 nm to 900 nm with increments of 2 nm. Images were obtained at every 2nm increment of wavelength starting from 650 nm and ending at 900 nm. Thus we get a 3-D Hyperspectral Image cube with 2 spatial dimensions and one spectral dimension. These cubes were obtained for each three different concentrations and also for spectralon (100 % reflectance). Each of these concentration cubes were then divided by the spectralon cube to obtain absorption of different ICG concentration. The resultant cube was then filtered using savitsky-golay filter and spectrum was plotted by taking a sample area from the cube that matches the position of the capillary. The calculated apparent absorption spectrum is shown below:

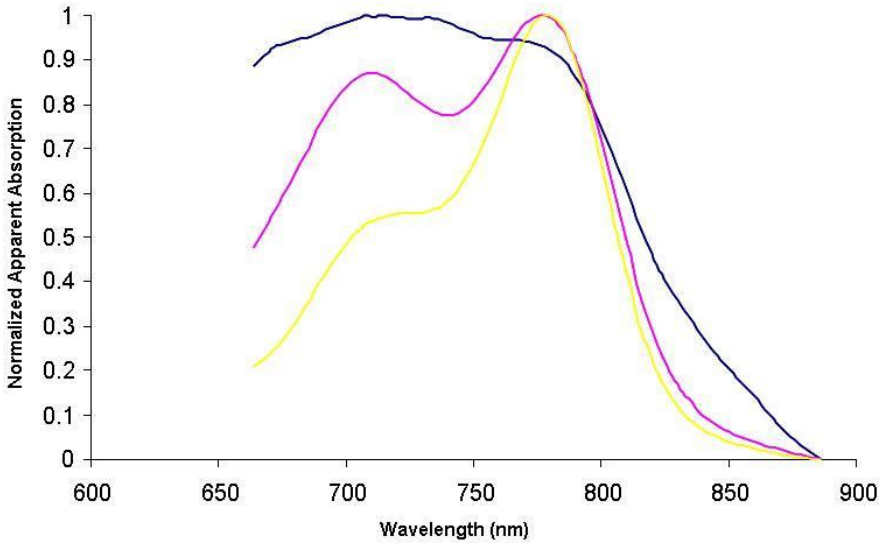

Figure 3.6: Normalized apparent absorption spectrum of different concentration of ICG in distilled water.Blue: Concentration 0.078 mg/ml, Pink: Concentration 0.015 mg/ml, Yellow: Concentration 0.005 mg/ml

Results:

From Fig 3.6 above we can conclude that ICG in distilled water has a bimodal peak absorption spectrum with maximum absorption occurring at 705 nm and 775 nm respectively. One important observation is the change in the shape of the curves with changes in concentration. We can clearly see that as we increase the concentration of ICG in distilled water, the peak at 775 nm tends to become a shoulder and the only one peak (705 nm) remains and as one decreases the concentration vice versa happens i.e. the peak at 705 nm tends to be a shoulder and only one peak 775 nm remains. This effect could be attributed to the aggregate formation of ICG when the concentration goes higher[15].

3.3 Best Concentration for Flourescence

Determination of fluorescence concentration that produces the best emission was required. The set up for determination of best fluorescence concentration is shown in the Fig 3.7.

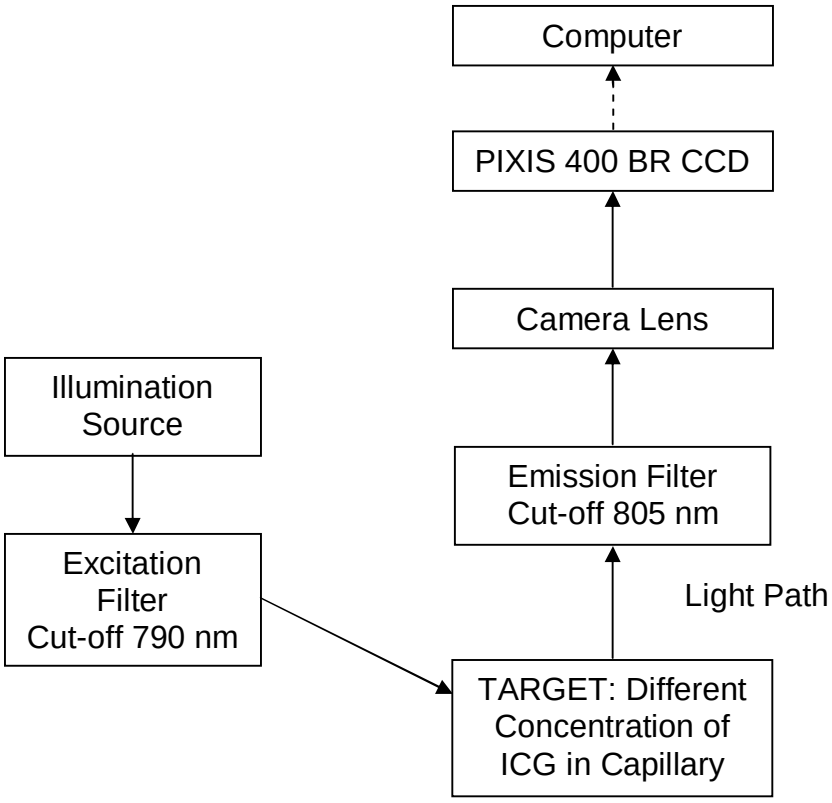

Figure 3.7: Block diagram depicting the set up used for measuring the best concentration of ICG in Water

Method:

A QTH source is coupled to a low pass filter (Cutoff 790 nm), providing with all excitation wavelength for ICG. Different concentrations of ICG in distilled water were used. 0.03mg/ml of ICG was first made by carefully measuring from Adventurer^{TM} (Ohaus). This solution was further diluted till all the other concentrations (0.02 mg/ml, 0.015mg/ml, 0.010 mg/ml, 0.005 mg/ml) were obtained. These solutions were put in different capillaries. An NIR detector (PIXIS 400BR) was coupled to an emission filter (CutOff (50%) 805nm) was used to measure the fluorescence. The 5 capillaries were kept parallel to each other and were excited by the QTH source coupled to the excitation filter as mentioned previously. Care was taken to make sure that the capillaries would almost

have the same intensity, by keeping the capillaries closer to each other. Fluorescence photons emitted by ICG were then detected using the detector mentioned above. Best concentration was decided based on the maximum fluorescence photons detected by the detector. Higher concentrations were eliminated as there was a reduction in fluorescence emission and due to restrictions on the dosage[29].

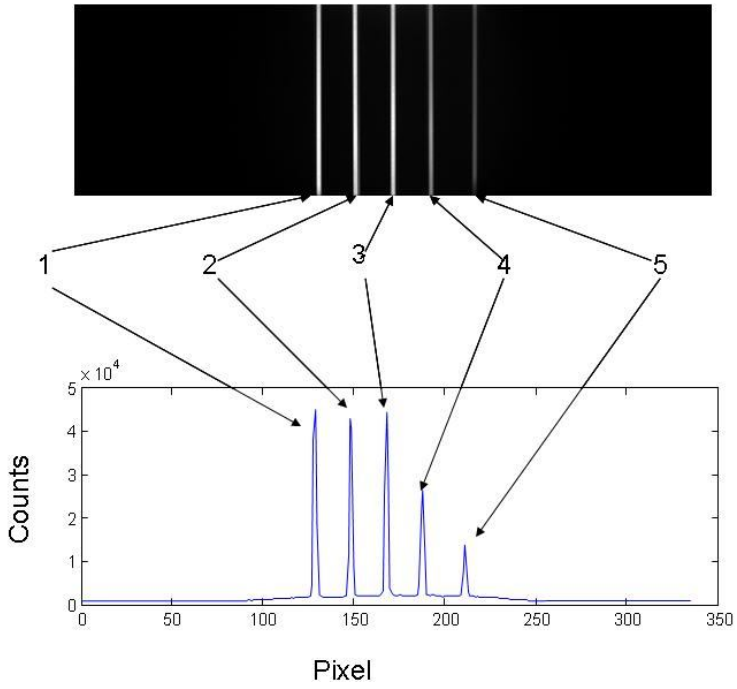

Figure 3.8: The above figure shows 5 capillaries containing different concentrations of ICG in distilled water. The plot below shows an average profile of the image above taken across columns. The Concentrations are 0.03 mg/ml, 0.02 mg/ml, 0.015 mg/ml, 0.010 mg/ml, and 0.005 mg/ml (Left to Right)

Results:

From the Fig 3.7 it is evident that fluorescence for 0.03 mg/ml, 0.02 mg/ml, 0.015 mg/ml are almost similar with peak fluorescence at 0.03 mg/ml and 0.015 mg /ml. Thus we could use either concentration for injecting into humans. However dosage regulations [29] restrict the concentration to 0.015 mg/ml. At higher concentrations ICG forms

aggregate. The total dose of dye injected should be kept below 2mg/kg. Thus for an average adult (weight: 70kg), the concentration of dye with blood as solvent would be 0.025 mg/ml. From the plot obtained in Fig 3.8, the best concentration lies within the limits of dosage prescribed.

3.4 Depth Analysis

One of the primary problems was determination of maximum depth of fluorescence inside tissue. Human tissue has both scattering and absorbance properties. Thus light falling on tissue gets partly scattered and partly absorbed. This depends on the absorbing properties of tissue. Different tissues have different absorption and scattering properties.

As discussed earlier one of the issues related to viewing the bile duct was that the CBD lies underneath a thick fat layer. Thus it is important to determine the depth that the fluorescence imager could see, to enable us to accurately determine the position of bile duct.

Method:

An intralipid model was considered, which would mimic tissue properties. A 1% intralipid solution was prepared by diluting 20% intralipid solution, obtained from Fresenius-Kabi, with distilled water. This 1% intralipid solution would mimic the properties of skin tissue[14]. 0.03 mg of ICG was carefully weighed using Adventurer™ (Ohaus) and mixed with 10 ml of distilled water. This solution was then diluted to get a concentration of 0.015 mg/ml. This fresh solution was ICG was filled into capillaries (1.5 mm Bore Diameter) using a 1 cc syringe. The capillary was then fitted to a stand, which

was coupled to a vernier height gage such that the capillary could be moved with precision in the vertical direction. The vernier height gage enables us to produce data at each millimeter. The fresh intralipid, prepared before was filled into a tub. The setup was arranged in such a way that the center point of the bore of the capillary was at the surface of 1% intralipid solution. A QTH source coupled with the low pass excitation filter (cut off 795nm) was used as excitation source for ICG in the capillary. The detector (PIXIS 400 BR) was coupled to a high pass Emission filter in the front. The distance between the source target and the detector is also illustrated in the figure. A distance of 22 inches between source and target was fixed because of clinical constraints during cholecystectomy surgery. The detector was focused on the surface of the intralipid. At each step the capillary was carefully moved into the intralipid in increments of 1 mm using the vernier scale. Care was taken not to disturb the alignment of the capillary tube with respect to the detector. Two different experiments were done using the same setup,

1. With constant exposure time: In this method the exposure time and aperture of the detector was adjusted to measure maximum fluorescence without getting saturated, when the ICG filled capillary was at the surface of intralipid. The same exposure time and aperture were used for all the depths. Background (Plain intralipid using both filters) images were also collected using the same exposure and aperture.
2. With variable exposure time: In this method, the exposure time was varied at each depth to get maximum fluorescence photons out of ICG. Thus each depth had a different exposure time. This difference in exposure time was taken care during the analysis of images. Background (Plain intralipid using both filters) images were also

collected using same aperture but different exposure to obtain maximum counts from the intralipid solution.

The entire experiment was conducted in the dark to maximally avoid any stray light from the background into the detector.

Data acquisition was also taken from Beef fat. Data was taken with capillary having aqueous ICG, at 2 mm from the surface of fat and at 2 cm from the surface of fat. The second data point could be used as a threshold to figure the penetration depth in the intralipid model as shown in Fig 3.12.

Results:

Images at different depth were collected in both methods. Images collected using method 1 (With constant exposure), were ratioed with background image obtained with all parameters same. However in the case of method 2 (Variable exposure time), each image was first divided by its exposure time to obtain an Intensity/sec at each pixel. Background image was also divided by the corresponding exposure time and then the each image was ratioed with the processed background image. Ratioing with the background image removes any source patterns associated with the original images. Thus we could then have the processed fluorescence signal. Beef fat was obtained and a capillary filled with ICG having the optimal concentration obtained above at approximately 2 mm to 3 mm below the surface of fat. The images obtained are shown in fig 3.9.

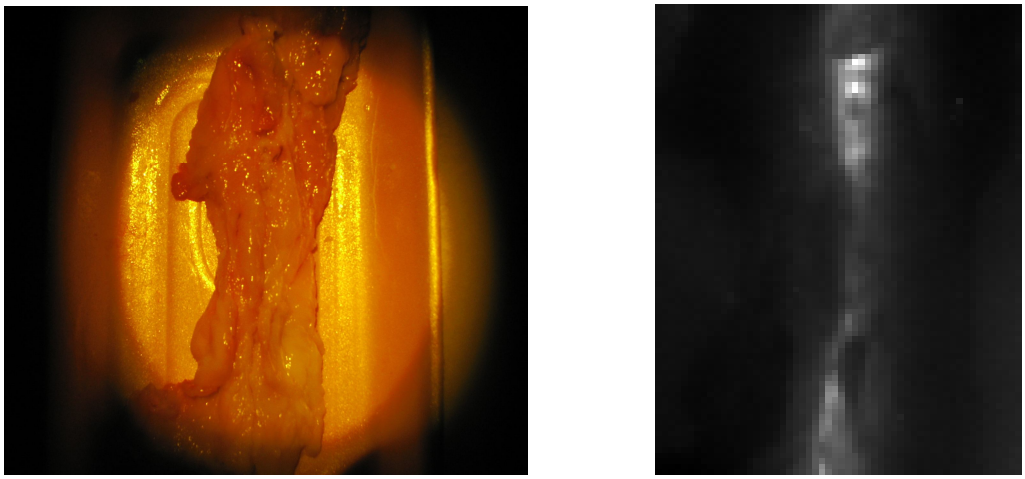

A B

Figure 3-9: Images of Beef fat with ICG in water filled capillary taken from two cameras (A) A digital Image of beef fat with capillary having ICG with water in it. (B) Image taken using the Surgical Fluorescence Imager of the same beef fat with capillary. The fluorescence glow can be clearly seen.

In both the methods, the processed images were then cropped for region of interest, and then a row profile of each row was obtained. This profile was median filtered with a filter window of 3. The signal to noise and contrast to background at each row were then averaged and plotted along with their error bars.

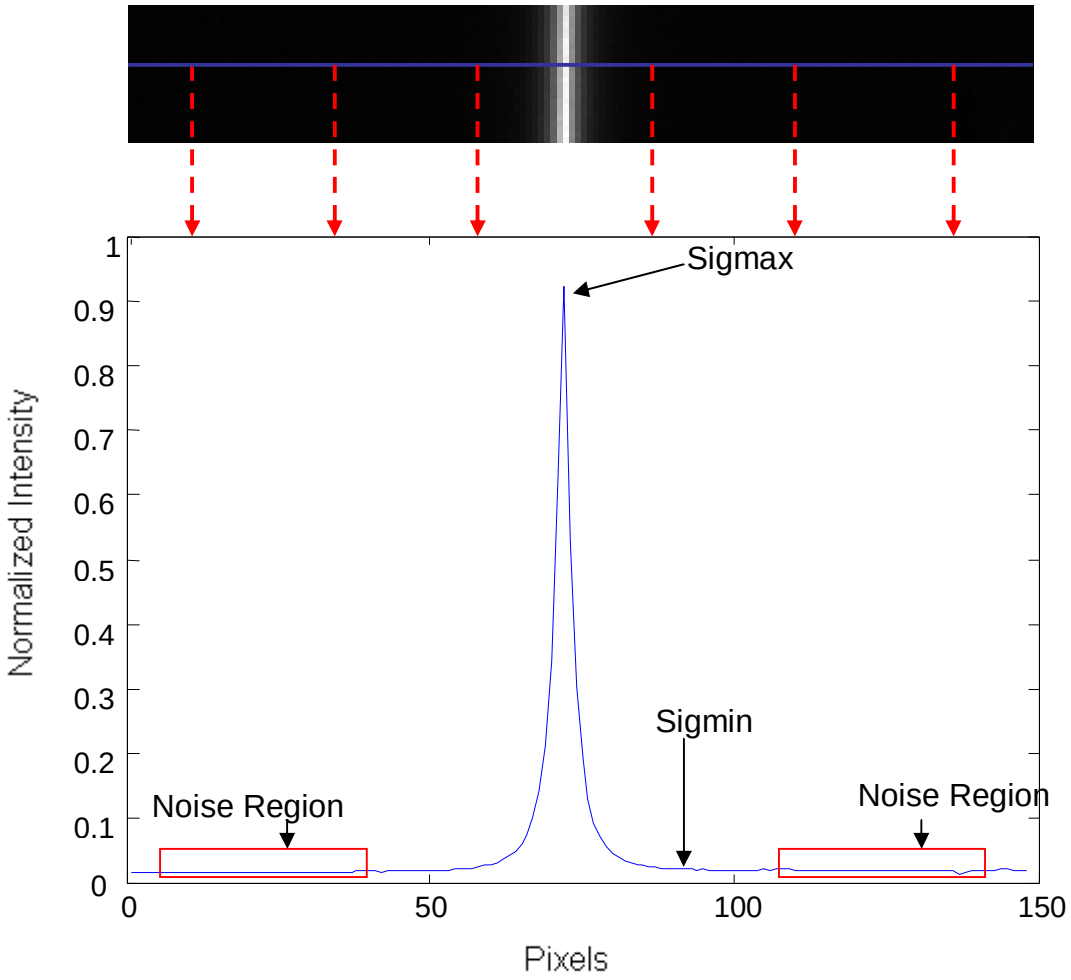

Figure 3.10: SNR and Contrast to Background Calculation. The profile is taken from each row of the image. SNR and contrast to background are then calculated for each row and then averaged

SNR Calculation:

SNR (Signal to Noise Ratio) is the ratio of signal power to the noise power. From the profile obtained above signal to noise was calculated by selecting the noise region, getting the standard deviation and then dividing the signal by this noise. This is depicted in the figure.

SNR = (Sig_{max} - Sig_{min} / Standard Deviation of the Noise Region)

Where Sig_{max} is the maximum fluorescence signal,

Sig_{min} is the baseline fluorescence signal.

The plots for both of these using both the above mentioned methods are shown below. SNR was calculated for each row from the cropped, processed image. A Mean SNR was calculated along with the standard deviation.

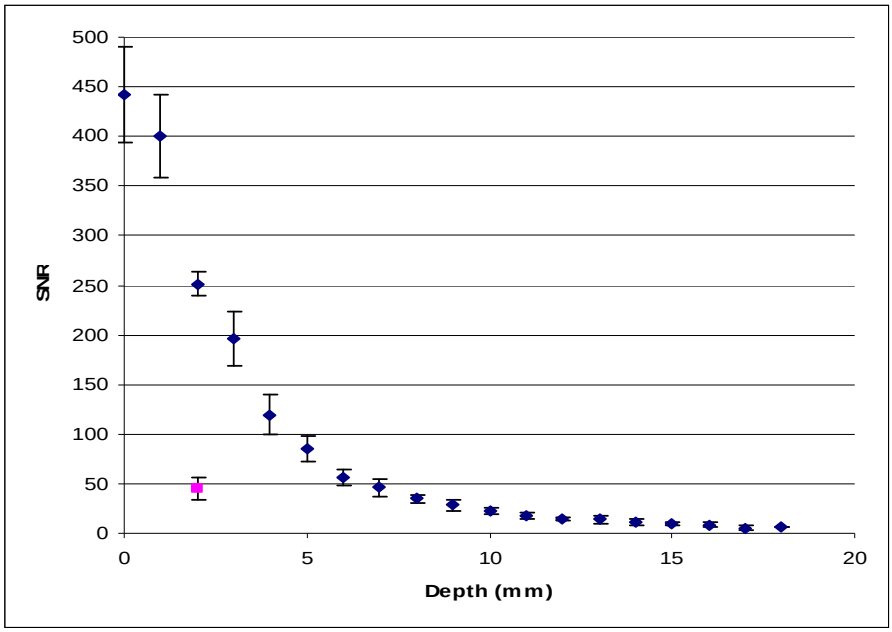

(A)

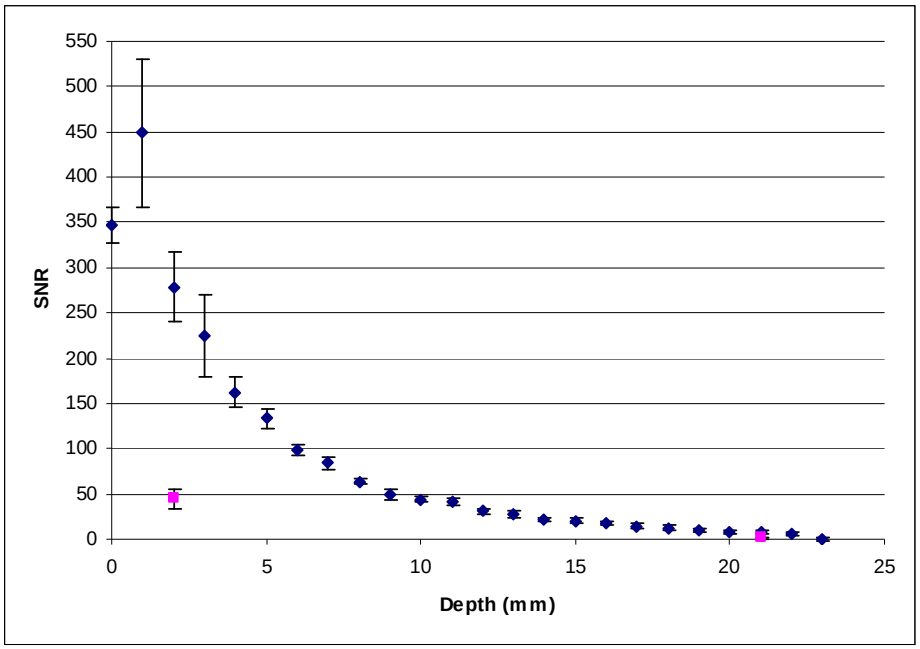

(B)

Figure 3.11: Plots depicting the signal to noise ratio against penetration depth in intralipid of Aqueous ICG. (A) With Constant Exposure. (B) With variable exposure. Pink data point: Data with aqueous ICG in beef fat at two different depths

From the Fig 3.10, we can see that the signal to noise decreases as the capillary goes deeper. As discussed earlier, intralipid has both absorption and scattering properties. When the fluorescence signal goes deeper, scattering and absorption takes place in the intralipid leading to lower signal and higher noise. Another factor that could affect the signal is the excitation source. Penetration depth of the excitation light itself could be lower due to intralipid absorption and scattering, thus leading to lower fluorescence signal, hence reduction in SNR. Typically the threshold for SNR is taken as 5. We can see from the plot that an SNR of 5 is reached at 18 mm below the surface with constant exposure and 21 mm depth with variable exposure.

Another measure of depth analysis, with the same set up was taken for ICG with bile. Care was taken to maintain the concentration of ICG in bile to be 0.015 mg/ml. This was carried out with constant exposure.

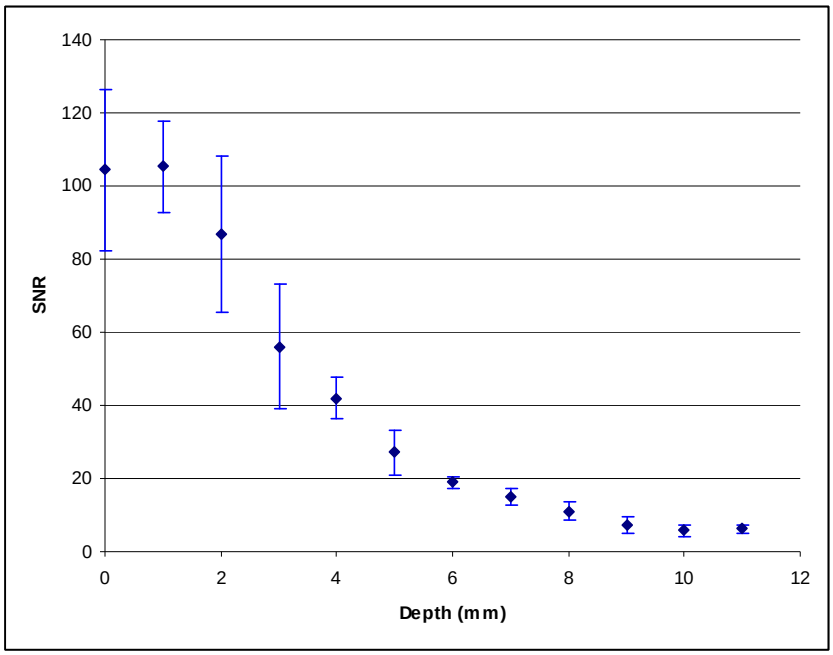

Figure 3.12: Plot depicting the signal to noise ratio against penetration depth in intralipid of ICG with Human Bile with Constant Exposure.

When Bile is mixed with ICG, the penetration depth reduces due to effects of the bile, like Quenching. Thus from the plot, we could see that an SNR of 5 is reached at 11 mm below the surface. Beyond this depth, it was difficult to distinguish between signal and noise hence data analysis had to be terminated.

Contrast to Background Calculation:

Contrast to Noise was calculated using the same value of signal as for SNR and dividing it by the mean of the noise region. This parameter could also be used as a deciding factor for finding the penetration depth of ICG in intralipid. The plots for contrast to background is shown below,

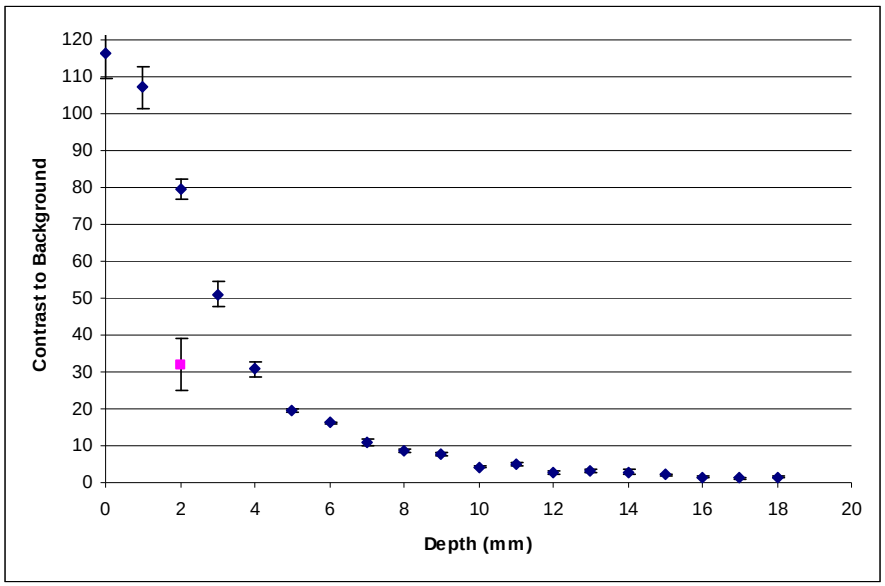

(A)

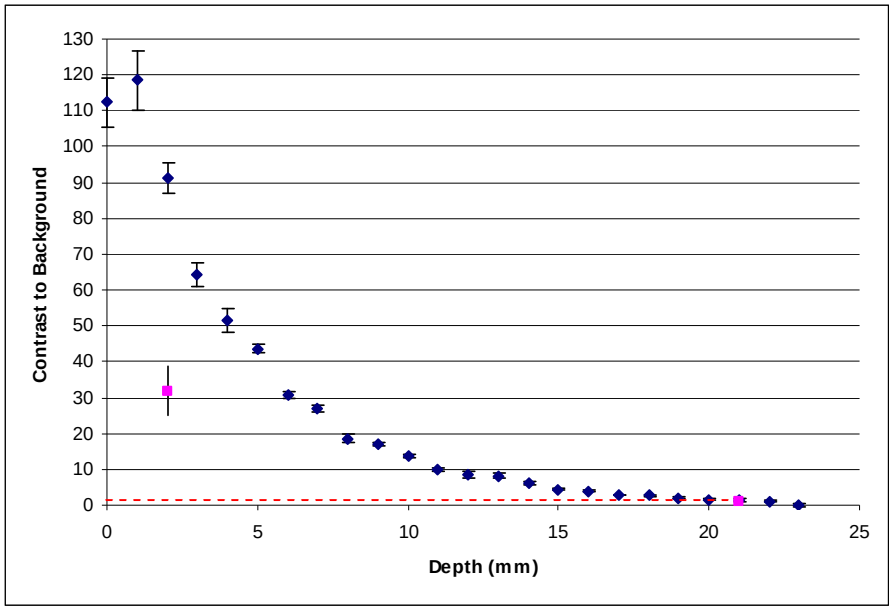

(B)

Figure 3.13: Plots depicting the Contrast to Background ratio against penetration depth in intralipid of Aqueous ICG. (A) With Constant Exposure. (B) With variable exposure. Pink data point: Data with aqueous ICG in beef fat at two different depths

Similar to Signal to Noise, contrast to background ratio was also computed for ICG with Bile in Intralipid solution,

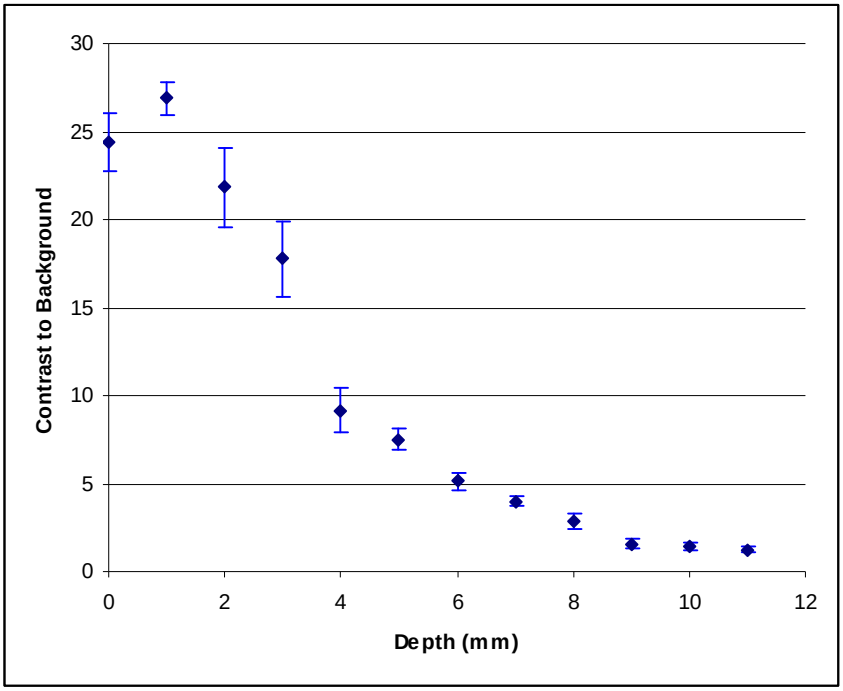

Figure 3.14: Plot depicting the Contrast to Background ratio against penetration depth in intralipid of ICG with Human Bile under Constant Exposure.

From the plot it can be perceived that the Contrast to Background ratio decreases with penetration. From Fig 3.12, we can conclude that the penetration depth of ICG with water in a 1% intralipid solution is approximately 21mm from the surface of intralipid. The red line in the plot determines the threshold value of contrast to background taken from aqueous ICG in beef fat. However since 1% intralipid solution is a homogenous medium and ICG in aqueous solution is also homogenous, the penetration depth would be high. Analysis of beef fat revealed and contrast to noise threshold of 1.0.

From Fig 3.13 we can see that the penetration depth is approximately 11 mm below the surface of intralipid beyond which the contrast to background ratio is below 1.

CHAPTER 4

FLUORESCENCE IMAGER USING BILIRUBIN

Bilirubin is one of the constituents of bile. It is one of the major organic product of heme catabolism: it is a yellow tetrapyrrole pigment that possesses two propionic side chains, which might be expected to render it highly polar and hence soluble in water. Due to internal hydrogen bonding, the bilirubin molecule can adopt a variety of configurations that render bilirubin poorly soluble in water. It is solubilized by interactions with micelles of bile salts and lipids in bile. In bile, bilirubin mostly exists as conjugated bilirubin. Unconjugated bilirubin amounts to 5% of total bilirubin[31].

Free bilirubin does not have high fluorescence. But conjugated bilirubin has a better quantum yield. The molecular structure of bilirubin is shown in the fig 4.1 below.

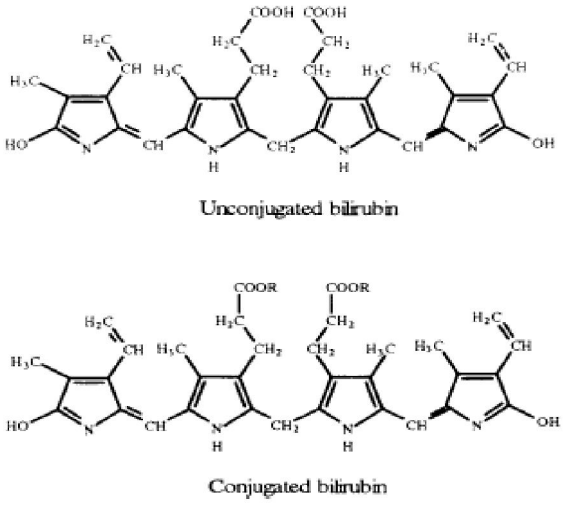

Figure 4.1: Molecular Structure of Conjugated and Unconjugated Bilirubin

Bilirubin has a strong and main absorption spectrum in the visible region with wavelength ranging from 390 nm to 460 nm and a molar absorption coefficient of approximately 50 x103 lmol-1cm-1 in aqueous solvents. The position of maximum, the shape of the spectrum and the molar absorption coefficient depends greatly on the conformational structure.

4.1 Fluorescence of Bilirubin

As discussed previously, free bilirubin shows a little fluorescence. However the fluorescence of bilirubin increases in the presence of albumin[32]. Bilirubin dianions combine reversibly with human albumin in neutral or alkaline solution[40]. bilirubin albumin solution has an absorption spectrum from 500 nm – 600 nm, with an emission occurring at around 528 nm.

Method:

Measurement of fluorescence was done using the source detector combination as shown in the figure below.

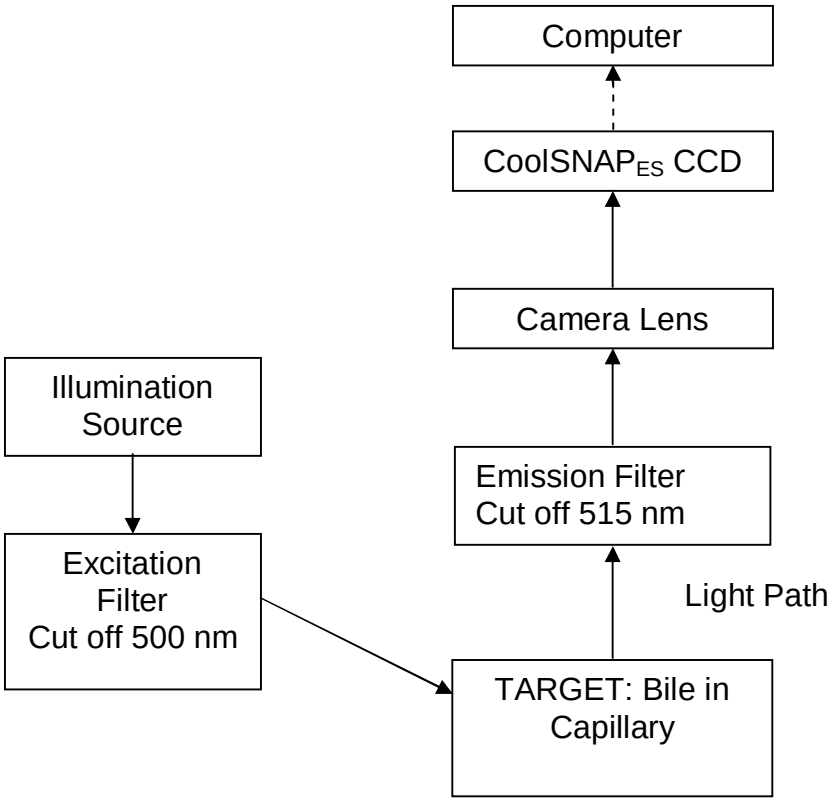

Figure 4.2: Block diagram depicting set up for measurement of fluorescence from Bilirubin

Bile was taken from the patient with the patient's consent. The raw bile was used for filling the capillary through a syringe. The capillary was kept over a black cloth to avoid any reflection coming as this would affect the fluorescence. The source is coupled to an excitation filter (Short Pass Cut off 500 nm) is used to excite the bile inside the capillary. The source is a broad band QTH source as discussed before. The source-filter combination is at a distance of 15" from the capillary. The detector used here is CoolSnap$_{ES}$ from Princeton instruments. The detector is coupled to the bilirubin emission filter (Long Pass Cut off 515 nm) along with a 50 mm/ F 1.4 Nikorr Lens. The detector and the source are arranged in reflective mode geometry as shown in fig 4.2. The detector is further connected to the laptop for data acquisition. In such a mode light emitted

through fluorescence is collected at the detector which then amplifies and gives the image.

Results:

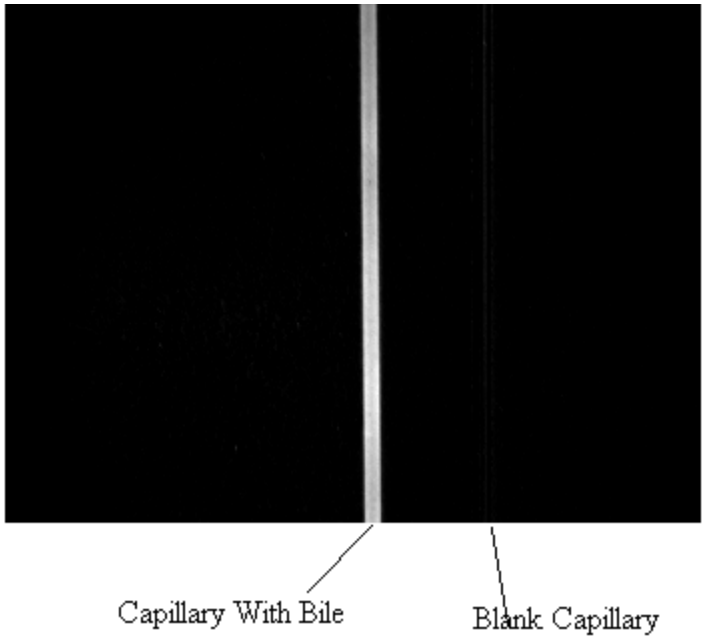

Figure 4.3: Fluorescence image of bilirubin with excitation from 400 nm – 500 nm. The fluorescence is clearly seen as compared to the blank capillary.

The above image is obtained by subtracting the raw image against its background (Image without the bile capillary). From the image we can clearly view the fluorescence of bilirubin. This could be used as one of the parameters in the detection of biliary duct. From this one could clearly state that the bilirubin in the bile fluoresces. This could be used as another method of visualizing bile duct in cholecystectomy procedure.

4.2 Percent Contrast – Spatial Resolution

The spatial resolution of the bilirubin fluorescence imager was established in a similar manner as it was done for finding percent contrast using ICG fluorescence

imager. However CoolSNAPES was the detector used. Excitation (Cut off 500nm) and Emission filters (Cut off 515 nm) were used.

The results are plotted below.

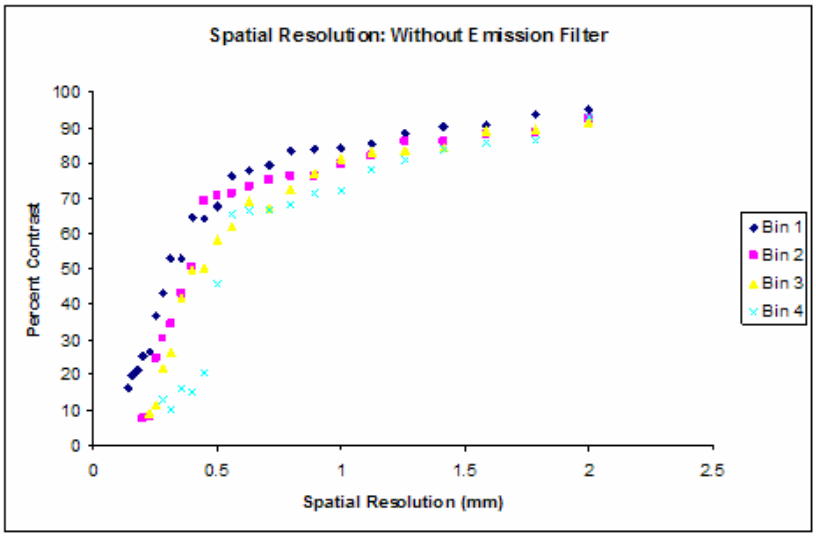

A

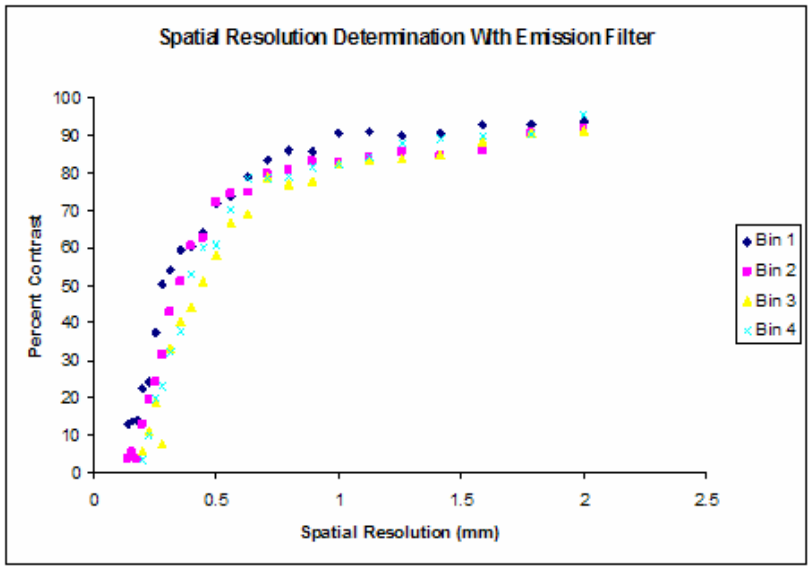

B

Figure 4.4: A. Plot depicting percent contrast against spatial resolution, when no emission filter is used B. Plot depicting percent contrast against spatial resolution, when emission filter is used

From Fig 4.4 (A) and (B) we can see that there is a slight decrease in the percent contrast when the emission filter is used in the path. This is possible as, there could be non-uniformity generated due to the filter from certain manufacturing issues. Also we can see that the spatial resolution with the emission filter is approximately .25mm (Percent Contrast 26%). This however does not reflect the spatial resolution when measuring fluorescence and just reflects the spatial resolution of the CCD coupled to the filter.

CHAPTER 5

CONCLUSION AND FUTURE GOALS

It has been demonstrated that Indocyanine Green and Bilirubin could be used as a latent contrast agent for visualizing anteriorly placed biliary structure. This is evident from the analysis of penetration depth in an intralipid model. However ICG mixed with bile resembles closer to real data imaging. Thus we could conclude that the penetration depth of Indocyanine Green would be approximately 11 mm below the surface of a 1% intralipid. From Fig 3.11 we can see that when plain aqueous ICG was used for depth analysis in 1% intralipid solution, the penetration depth is almost doubled. This proves that when bile is mixed with ICG, aggregates are formed. Also bile itself absorbs some of the incident radiation that falls on to it, reducing the excitation energy for ICG. However this forms a more realistic model that could be used for clinical studies.

Previous work with ICG illustrates the use of ICG as a potential contrast agent without exploiting its fluorescence properties. Future goal of this project would include imaging animals by injecting ICG into the body, which would increase the possibility of this system to be used as a device for clinical studies with humans.

One of the potential drawbacks of this system is the injection of an external agent into the body. So care would have to be taken for any person developing allergic reactions to contrast agents. Another drawback of the system is the time that ICG takes to reach the biliary structure. Vials of ICG are quite stable for a span of 5 hours[15]. It takes

about 120 to 150 minutes for ICG to reach the biliary structure[38]. Thus the patient will have to be injected with ICG approximately 150 minutes before the surgery.

The drawback regarding ICG could be overcome if bilirubin is used as a fluorophore. Bilirubin already exists in the body, requiring no injection or any potential problems regarding allergic reactions. Due to timely unavailability of human bile, penetration depth analysis could not be done with bilirubin.

Replacing the existing source-excitation filter combination with a DLP light source would make the system more precise and efficient.

REFERENCES

1. http://www.surgerychannel.com/cholecystectomy/index.shtml
2. http://en.wikipedia.org/wiki/Cholecystectomy
3. http://www.women-health-guide.com/cholelithiasis.htm
4. http://en.wikipedia.org/wiki/Cholecystitis
5. http://images.emedicinehealth.com/images/eMedicineHealth/illustrations/gallstones.jpg
6. http://www.mamashealth.com/organs/gallbladder.asp
7. http://www.umm.edu/patiented/articles/what_symptoms_of_gallstones_gallbladder_disease_000010_2.htm
8. http://www.roper.co.jp/Html/roper/ps_pixis/pdf/pixis_400br.pdf
9. http://www.roperscientific.com/manuals/coolsnapcf/57061001.pdf
10. 'The Newport Resource' 2008-2009. Newport Corporation pp 137 - 138
11. 'The Newport Resource' 2008-2009. Newport Corporation pp 140 - 141
12. http://www.newport.com/file_store/Supporting_Documents/Tech_Ref_Spectral_Irradiance37.pdf
13. 'The Newport Resource' 2008-2009. Newport Corporation pp 132

14. I Driver, J W Feather, P R King, J B Dawson “The optical properties of aqueous suspensions of Intralipid, a fat emulsion” Phys. Med. Biol., 1989 Vol:34, No 12, 1927- 1930
15. M. L. J. Landsman, G. Kwant, G. A. Mook, W. G. Zijlstra, “Light- Absorbing Properties, Stability and Spectral Stabilization of Indocyanine Green”, Jour. Applied Physiology, Vol. 40, No. 4, April 1978
16. R.C. Benson, H. A. Kues, “Fluorescence properties of Indocyanine Green as Related to Angiography”, Vol. 23, No. 1, 159-163, Phys. Med. Biol. 1978
17. http://akorn.com/documents/catalog/package_inserts/17478-701-02.pdf
18. M.A. Rosci, “Fluorescence of free bilirubin at room temperature”, Experimentia Vol: 39 (1983)
19. http://www.nikonusa.com/Find-Your-Nikon/ProductDetail.page?pid=1902
20. http://en.wikipedia.org/wiki/Charge-coupled_device
21. PIXIS User Manual.
22. http://content.piacton.com/Uploads/Princeton/Documents/Datasheets/PIXIS/PIXIS%20400%20Rev%20B0.pdf
23. http://content.piacton.com/Uploads/Princeton/Documents/Whitepapers/etaloning.pdf
24. http://www.piacton.com/pdfs/whitepapers/interline.pdf
25. CoolSnap$_{ES}$ user manual
26. http://www.photomet.com/pm_downloads/software_pvcam.php
27. http://www.photomet.com/pm_solutions/library_encyclopedia/index.php
28. http://omlc.ogi.edu/spectra/icg/index.html

29. http://www.akorn.com/documents/catalog/package_inserts/17478-701-02.pdf
30. Gilbert R. Cherrick, Samuel W. Stein, Carroll M. Leevy, Charles S. Davidson "Indocyanine Green: Observations on its physical properties, plasma decay and hepatic extraction"
31. Francesco Baldini, Paolo Bechi, Fabio Cianchi, Alida Falai, Claudia Fiorillo, Paolo Nassi "Analysis of Optical Properties of Bile" J. Biomedical Optics 5(3), 321-329, July 2000
32. Humra Athar, Nisar Ahmad, Saad Tayyab, Mohammad A. Qasim "Use of Fluorescence enhancement technique to study bilirubin-albumin interaction" Int. J. Biological Macromolecules, 25, 353-358, 1999
33. Mirizzi PL. 1937 Operative Cholangiography Surg Gynaecol Obstet. 1937 ; 65; 702-710
34. Qasim Al-qasabi et al. "Operative Cholangiography in Laproscopic Cholecystectomy: Is it essential"
35. A Persson, N Dahlström, Ö Smedby and TB Brismar : "Three-dimensional drip infusion CT cholangiography in patients with suspected obstructive biliary disease: a retrospective analysis of feasibility and adverse reaction to contrast material"
36. Flowers JL, Zucker KL, Graham SM, et al. "Laparoscopic cholangiography: results and indications." Ann Surg 1992; 215:209-16.
37. Gerber A, Apt MK. "The case against routine operative cholangiography. AM J Surg" 1982; 143:734-6.

38. Araki, K. Namikawa, J. Mizutani, M. Doiguchi, H. Yamamoto, Arai T. Yamaguchi, et al. “Indocyanine Green Staining for Visualization of Biliary System during Laparoscopic Cholecystectomy”.
39. D. Persemlidis, A. Barzilai, et al. “Enhanced Laparoscopic Visualization of Extrahepatic Bile duct with Intravenous ICG”
40. Jorgen Jacobsen, Rolf Broderson “Albumin- Bilirubin Binding Mechanism” Jour. Of Biological Chemistry, Vol 258, No.10, Issue of May 25, pp. 6319-6326, 1983

BIOGRAPHICAL INFORMATION

Santosh Hariharan was born in Mumbai, India and has to his credit a Bachelor's degree from National Institute of Technology, Calicut, India conferred in May 2004. He joined the University of Texas Arlington for his Master's degree in Biomedical Engineering in August 2006. His research interest lies in the field of optical imaging concentrating on Hyperspectral imaging and Fluorescence imaging for developing non-invasive systems for clinical use.